

Contract No:

This document was prepared in conjunction with work accomplished under Contract No. DE-AC09-08SR22470 with the U.S. Department of Energy (DOE) Office of Environmental Management (EM).

Disclaimer:

This work was prepared under an agreement with and funded by the U.S. Government. Neither the U. S. Government or its employees, nor any of its contractors, subcontractors or their employees, makes any express or implied:

- 1) warranty or assumes any legal liability for the accuracy, completeness, or for the use or results of such use of any information, product, or process disclosed; or
- 2) representation that such use or results of such use would not infringe privately owned rights; or
- 3) endorsement or recommendation of any specifically identified commercial product, process, or service.

Any views and opinions of authors expressed in this work do not necessarily state or reflect those of the United States Government, or its contractors, or subcontractors.



Savannah River
National Laboratory®

A U.S. DEPARTMENT OF ENERGY NATIONAL LABORATORY • SAVANNAH RIVER SITE • AIKEN, SC

Component-In-Grout Model Implementation for the E-Area Low-Level Waste Facility's Performance Assessment

T. L. Danielson

September 2020

SRNL-STI-2020-00365, Revision 0

SRNL.DOE.GOV

DISCLAIMER

This work was prepared under an agreement with and funded by the U.S. Government. Neither the U.S. Government or its employees, nor any of its contractors, subcontractors or their employees, makes any express or implied:

1. warranty or assumes any legal liability for the accuracy, completeness, or for the use or results of such use of any information, product, or process disclosed; or
2. representation that such use or results of such use would not infringe privately owned rights; or
3. endorsement or recommendation of any specifically identified commercial product, process, or service.

Any views and opinions of authors expressed in this work do not necessarily state or reflect those of the United States Government, or its contractors, or subcontractors.

Printed in the United States of America

**Prepared for
U.S. Department of Energy**

Keywords: *Groundwater Modeling*
Performance Assessment
Cementitious Wasteforms

Retention: *Permanent*

Component-In-Grout Model Implementation for the E-Area Low-Level Waste Facility's Performance Assessment

T. L. Danielson

September 2020

Prepared for the U.S. Department of Energy under
contract number DE-AC09-08SR22470.



REVIEWS AND APPROVALS

AUTHORS:

T. L. Danielson, SRNL, Environmental Sciences & Dosimetry Date

TECHNICAL REVIEW:

L. L. Hamm, SRNL, Advanced Modeling and Simulation Date

B. T. Butcher, SRNL, Environmental & Biological Sciences Date

APPROVAL:

D. G. Jackson, Manager Date
SRNL, Environmental Sciences & Dosimetry

B. D. Lee, Manager Date
SRNL, Environmental & Biological Sciences

EXECUTIVE SUMMARY

The component-in-grout (CIG) disposal units are below grade earthen trenches that contain grout encapsulated waste components. Components disposed of within the CIG segments consist of large radioactively contaminated equipment and smaller waste forms (e.g., B-25 boxes and SeaLand containers) to fill the space around and above the large equipment. In the 2022 revision of the E-Area Low-Level Waste Facility's (ELLWF) performance assessment, groundwater radionuclide contaminant transport through the vadose zone will be modeled using the PORFLOW software package for nine existing CIG segments located within the Slit Trench (ST) 23 footprint – no additional CIG segments are planned for at this time. The nine CIG segments have been placed within two of the nominally 20-foot-wide by 656-foot-long ST segments and are surrounded by no less than 1 foot of grout on all sides and up to 4 feet of backfill material. The two most recently placed CIG segments have an additional reinforced concrete mat to improve structural stability.

The current report details the key inputs and assumptions for developing a conceptual model of groundwater radionuclide contaminant transport through the vadose zone from existing CIG segments in the ELLWF. Groundwater modeling consists of the sequential calculation of time varying, steady-state flow fields that serve as inputs for radionuclide contaminant transport simulations carried out in PORFLOW. Water infiltration rate boundary conditions for each flow field account for four distinct time periods: the operational period (i.e., no cover), the operational closure period (i.e., the placement of an operational runoff cover), the interim closure period (i.e., the placement of an interim closure cover that extends across the facility and maintenance requirements remain in place), and the final closure period (i.e., where a low permeability, multi-layer soil-geomembrane final closure cap is placed and no maintenance requirements remain in place). In addition to the intact cover conditions, four CIG segments (CIG-4 through CIG-7) have been identified as having non-negligible subsidence potential. To account for this, subsidence infiltration boundary conditions have been modeled for two cases: the conservative base case where subsidence occurs immediately at the time of final closure and the best-estimate case where subsidence occurs 200 years post-closure. The flux-to-the-water-table profiles for each radionuclide will act as source terms at the water table during radionuclide transport through the aquifer allowing calculation of the predicted dose through various pathways.

TABLE OF CONTENTS

LIST OF TABLES	vii
LIST OF FIGURES.....	vii
LIST OF ABBREVIATIONS.....	ix
1.0 Introduction.....	1
2.0 Key Inputs and Assumptions.....	2
2.1 Model Geometry	3
2.2 Timeline and Boundary Conditions	4
2.3 Physical and Chemical Properties	7
3.0 Results and Discussion	10
3.1 Preliminary Flow Results	12
3.2 Preliminary Transport Results	23
4.0 Conclusions.....	31
5.0 References.....	32

LIST OF TABLES

Table 2-1. Date of first waste placement in each component-in-grout unit – relative times are rounded to the nearest integer year.	4
Table 2-2. Time-dependent water infiltration rate through the intact final closure cap as reported in Dyer (2019).	5
Table 2-3. Infiltration rates in inches/year for the bounding and best estimate cases for CIG-4 through -7.	7
Table 2-4. Upslope intact length and subsided region lengths used for calculating subsided infiltration rates.	7
Table 2-5. Material types applied to each material zone through time.	8
Table 2-6. Physical properties for each material type.	9
Table 2-7. Half-lives and K_d 's for the suite of radionuclides tested during implementation. Parent radionuclides are in bold and progeny are not bold.	10
Table 3-1. Temporal discretization of the performance assessment time period. First waste and the time to the operation cover are CIG-unit dependent (reference Section 2.2).	10
Table 3-2. Cementitious material aging times (simulation year referenced from the start of operations in the ELLWF) computed from the steady-state flow fields.	24

LIST OF FIGURES

Figure 1-1. Layout of disposal units within the E-Area Low-Level Waste Facility.	1
Figure 2-1. Nominal cross-sectional layout and design of CIG segments within a slit-trench footprint.	3
Figure 2-2. Material layout of cross-sectional model of component-in-grout unit.	4
Figure 2-3. Layout of as-built component-in-grout units 1 through 9 within the ST 23 footprint.	6
Figure 3-1. Saturation profile for CIG-4 during the operational period.	13
Figure 3-2. Saturation profile for CIG-4 during the operational closure period.	13
Figure 3-3. Saturation profile for CIG-4 during the interim closure period, prior to hydraulic degradation.	14
Figure 3-4. Saturation profile for CIG-4 during the interim closure period, after hydraulic degradation.	14
Figure 3-5. Saturation profile for CIG-4 at the end of institutional control.	15
Figure 3-6. Saturation profile for CIG-4 at 371 years.	15
Figure 3-7. Saturation profile for CIG-8 during the operational time period.	16
Figure 3-8. Saturation profile for CIG-9 during the operational time period.	16

Figure 3-9. Saturation profile for CIG-8 during the operational closure period. 17

Figure 3-10. Saturation profile for CIG-9 during the operational closure period. 17

Figure 3-11. Saturation profile for CIG-8 during the interim closure period, prior to hydraulic degradation.
..... 18

Figure 3-12. Saturation profile for CIG-9 during the interim closure period, prior to hydraulic degradation.
..... 18

Figure 3-13. Saturation profile for CIG-8 during the interim closure period, after hydraulic degradation.
..... 19

Figure 3-14. Saturation profile for CIG-9 during the interim closure period, after hydraulic degradation.
..... 19

Figure 3-15. Saturation profile for CIG-8 at the end of institutional control. 20

Figure 3-16. Saturation profile for CIG-9 at the end of institutional control. 20

Figure 3-17. Saturation profile for CIG-8 at 371 years. 21

Figure 3-18. Saturation profile for CIG-9 at 371 years. 21

Figure 3-19. Saturation profile for CIG-4 with subsidence at 171 years. 22

Figure 3-20. Saturation profile for CIG-4 with subsidence at 371 years. 23

Figure 3-21. C-14 flux to the water table from CIG-4. 25

Figure 3-22. H-3 flux to the water table from CIG-4. 25

Figure 3-23. Sr-90 flux to the water table from CIG-4. 26

Figure 3-24. I-129 flux to the water table from CIG-4. 26

Figure 3-25. Np-237 flux to the water table from CIG-4. 27

Figure 3-26. U-238 (and progeny) flux to the water table from CIG-4. 27

Figure 3-27. Tc-99 flux to the water table from CIG-4. 28

Figure 3-28. C-14 flux to the water table from CIG-4, -8, and -9. 28

Figure 3-29. H-3 flux to the water table from CIG-4, -8, and -9. 29

Figure 3-30. I-129 flux to the water table from CIG-4, -8, and -9. 29

Figure 3-31. Tc-99 flux to the water table from CIG-4, -8, and -9. 30

Figure 3-32. Sr-90 flux to the water table from CIG-4, -8, and -9. 30

Figure 3-33. Np-237 flux to the water table from CIG-4, -8, and -9. 31

LIST OF ABBREVIATIONS

SRNL	Savannah River National Laboratory
CIG	Component-in-Grout
ELLWF	E-Area Low Level Waste Facility
ST	Slit Trench
PA	Performance Assessment

1.0 Introduction

The component-in-grout (CIG) disposal units are below grade earthen trenches that contain grout encapsulated waste components. Historically there were two CIG-designated trench units in the E-Area Low-Level Waste Facility (ELLWF). Over time, the CIG disposal methodology has become less favorable due to the high cost of disposition and the nature of contemporary waste streams (i.e., grout encapsulation is generally unnecessary). Thus, existing trench CIG01 and future trench CIG02 have been repurposed as Slit Trench 23 (ST23) and Slit Trench 24 (ST24) (Hamm 2019). The position of ST23 and ST24 relative to other trenches in the ELLWF is shown in Figure 1-1. To date, only nine CIG segments exist and were placed within two of the nominally 20-foot-wide by 656-foot-long trench segments within the ST23 footprint between 8/29/2000 and 6/26/2007. Since that time, the remaining volume of the trench footprint has been re-allocated for standard Slit Trench (ST) waste. Any future CIG disposals would therefore require a special analysis before placement.

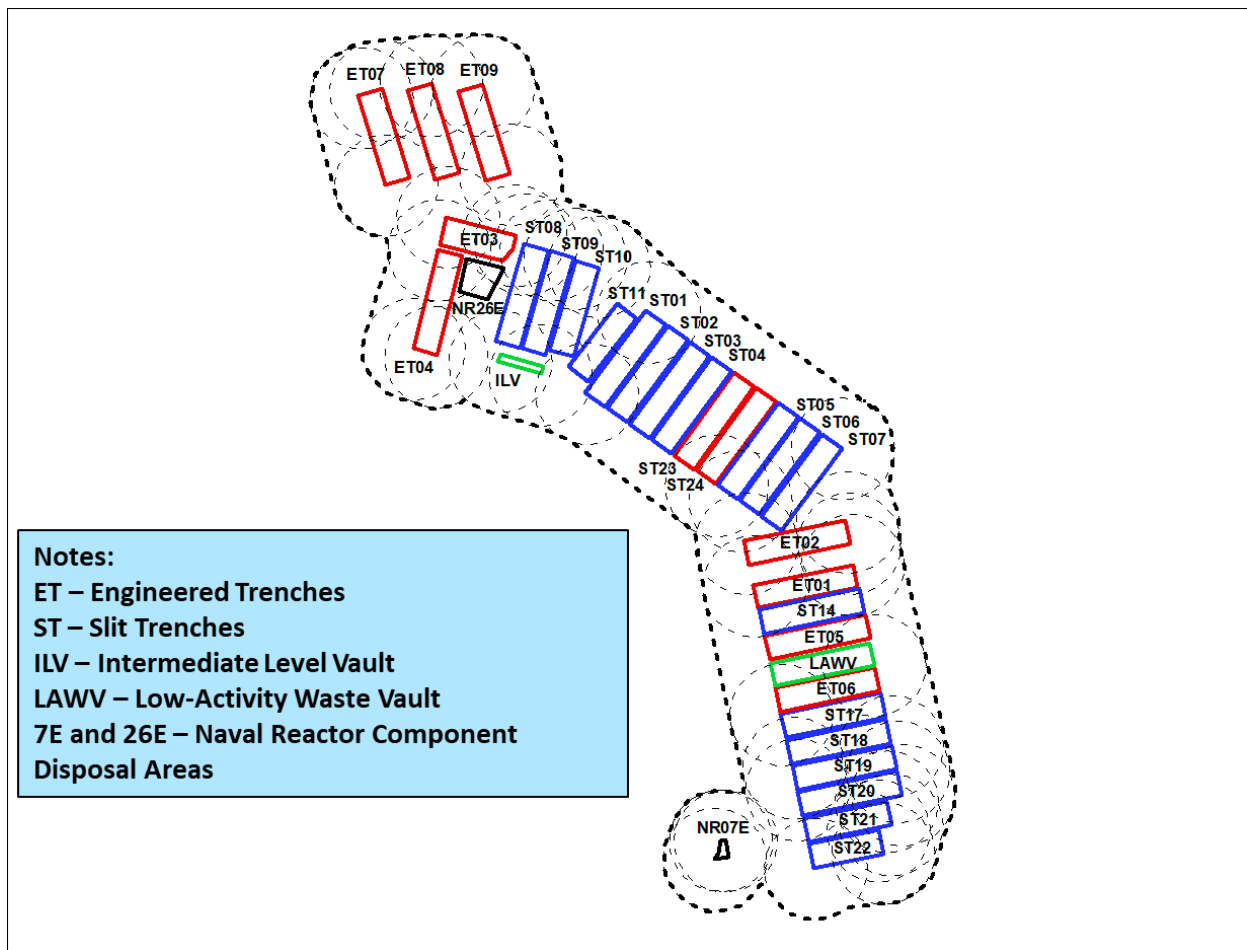


Figure 1-1. Layout of disposal units within the E-Area Low-Level Waste Facility.

The components that have been disposed of within the existing nine CIG segments (referred to as “units” in this report) include large radioactively contaminated components such as tankers, radioactive sources from a concrete culvert, flatbed trailers, SeaLand containers, and various high integrity containers. In addition, other waste forms such as B-25 boxes and B-12 boxes are placed around and above larger equipment to maximize use of the disposal volume and eliminate void space. CIG units have been excavated as needed and the unit numbers are designated sequentially in order of placement [e.g., CIG unit

1 (CIG-1) was created first and CIG unit 9 (CIG-9) last]. CIG units are nominally 20 feet deep, though in practice, are excavated only to the necessary depth and length for the component(s) to reduce the cost associated with grouting. Excavated soil from the unit is set aside for later use as backfill material. Before waste placement, the base of the CIG unit is filled with a high flow grout to a minimum of one-foot thickness and the grout is allowed to solidify after which, components are placed and grout is poured around, between, and over to encapsulate. Waste is placed such that a one-foot grout encapsulation layer (i.e., the same as the base) separates the grouted components from the soil along the sides of the trench segments. Additional components or other waste forms can be placed on top of previously grouted components up to a maximum height of 15 feet such that a one-foot grout encapsulation layer can be placed over top to separate waste from the backfill material.

The life cycle of the CIG units is carried out in accordance with the rest of the ELLWF starting with the operational period during which waste is placed. Once a CIG component is encapsulated, a minimum four feet of backfill material is placed in the remaining volume of trench space over top of the composite grouted waste form. The subsidence potential of CIG units is highly variable. Two units, CIG-8 and CIG-9, have had a reinforced concrete mat placed over top of the composite grouted waste form to decrease the subsidence potential over time and therefore have less backfill material. Finally, an initial plastic cover is required to be installed over each newly completed CIG unit within three months of the component(s) being disposed to reduce infiltration. As previously mentioned, trench CIG01 is being repurposed as ST23 with the remaining space to be filled with ST waste. Upon operational closure of this entire ST, soil will be built up and grading performed over the trench to promote positive drainage, and an operational runoff cover is to be placed and maintained over the trench.

At the end of ELLWF operations, an integrated interim runoff cover is to be installed across all trenches (ET's and ST's) in the ELLWF marking the start of institutional control. The interim runoff cover and associated stormwater drainage system is assumed to be maintained for a period of 100 years.

Finally, after the 100-year period of institutional control a low permeability, multi-layer soil-geomembrane final closure cap is installed, preceded by dynamic compaction across trenches in the facility to reduce void space. No additional maintenance and loss of institutional memory is assumed during the 1,000-year post-closure period. As a result of these assumptions, subsidence (i.e., due to settling and degradation of waste forms) of the final closure cap will occur leading to increased water infiltration.

In the FY2022 revision of the ELLWF performance assessment (PA), groundwater radionuclide contaminant transport modeling will be executed in order to compute disposal limits based on the projected dose through various exposure pathways. The first modeling step involves deterministic simulations of radionuclide transport from the disposal unit of interest through the vadose zone such that a time dependent aquifer source term can be obtained for each radionuclide from the flux to the water table profile. The following sections describe the development of a conceptual model representative of the original nine units of CIG special wastefoms by employing the nominal CIG unit geometry (Section 2.1), operational timeline/closure sequence and boundary conditions (Section 2.2), and properties of the CIG disposal system materials (Section 2.3) in a PORFLOW-based flow and transport model. The radionuclide flux to the water table from these nine units will be inserted into the appropriate aquifer source cells beneath ST23 and combined with flux from generic ST waste sections of the trench for a representative flux to the water table for each radionuclide. In Section 3.0, preliminary vadose zone flow and transport results for the existing CIG units are presented based on the conceptual model's implementation in PORFLOW (ACRi, 2018).

2.0 Key Inputs and Assumptions

In Section 1.0, a high-level description of the CIG disposal units was presented to provide a foundational understanding for developing conceptual models to simulate the transport of radionuclides from the

composite cementitious waste form through the vadose zone. In the current section, the key inputs and assumptions for creating a generalized conceptual model for CIG disposal units in the ELLWF will be presented.

2.1 Model Geometry

In an effort to reduce the overall number of conceptual models, a generalized conceptual model geometry has been developed based on a two-dimensional cross-section of a CIG unit. The foundation for this model geometry is based on the nominal dimensions of a CIG unit as shown in Figure 2-1. The CIG units are nominally 20-feet wide and 20-feet deep with a 1-foot grout encapsulation layer on all sides. CIG units located alongside of adjacent ST segments are separated by a minimum of 10-feet of upper vadose zone clayey material. The impact of a neighboring trench unit on the flow of water around a CIG unit is considered negligible and therefore, only one segment is represented within the simulation geometry.

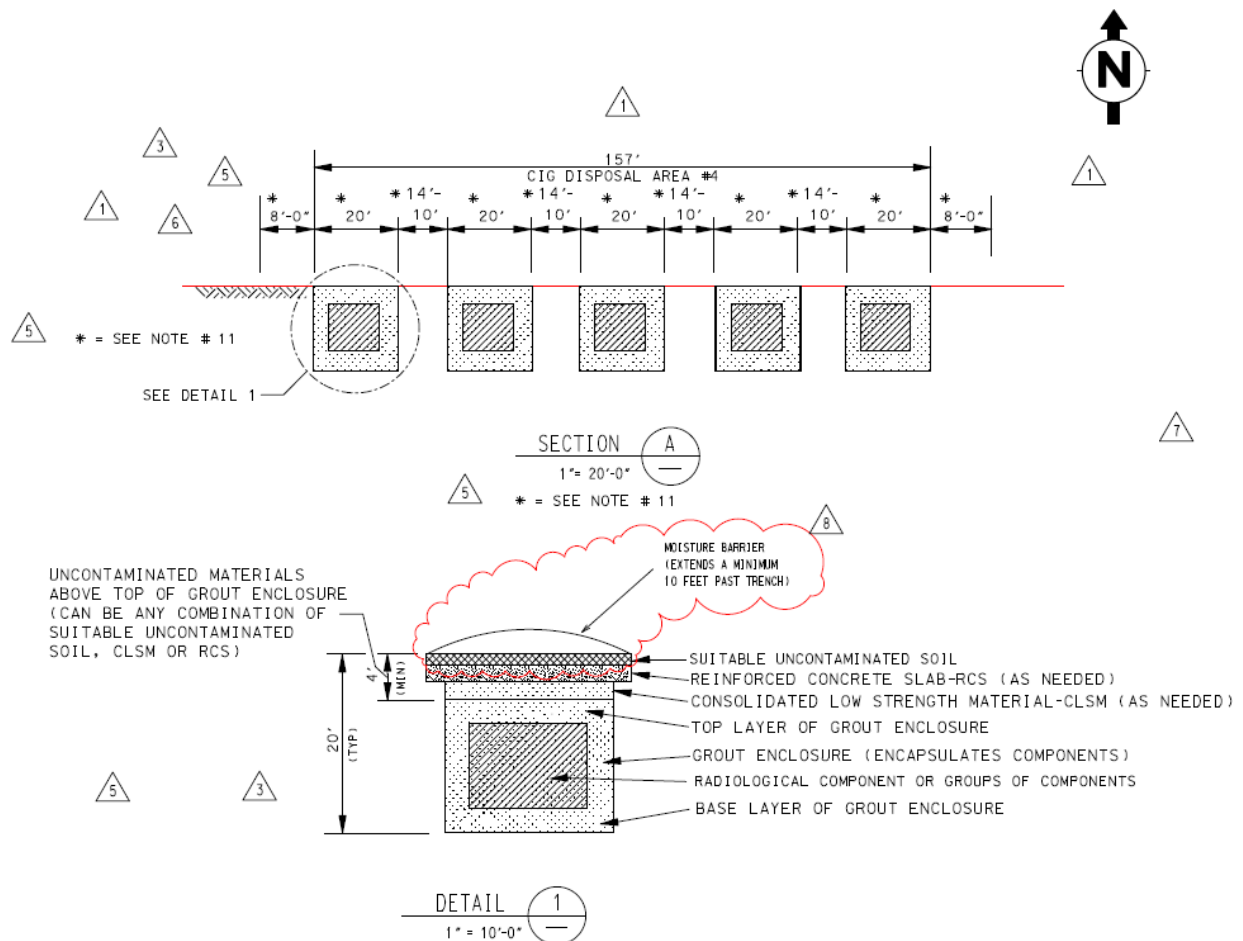


Figure 2-1. Nominal cross-sectional layout and design of CIG segments within a slit-trench footprint.

The cross-sectional material layout for the CIG unit model is shown in Figure 2-2. The hydrostratigraphic surfaces present around and beneath the CIG units are taken directly from Danielson (2019) and are based on the work of Bagwell and Bennett (2017). The thickness of grout surrounding the waste zone is 1-foot thick on all sides and the waste zone is 18 feet wide by 14 feet tall (excluding the grout encapsulating layer). The thickness of the CLSM and reinforced mat is 16 inches and 24 inches, respectively, and both span the width of the 20-foot trench segment. Notably, these two materials are only present if a reinforced concrete mat has been placed over the composite grout waste form (i.e., CIG-8 and CIG-9), otherwise, these material

regions are made up of a soil backfill (chemical and physical properties of the material regions are discussed in Section 2.3). The extent of the operational, interim, and final covers is shown in Figure 2-2, but is not modeled explicitly – only boundary conditions specifications (discussed in Section 2.2) are applied across these regions. The operational cover extends only 10 feet past the edge of the trench segment, whereas the interim and final covers extend across the entire model domain.

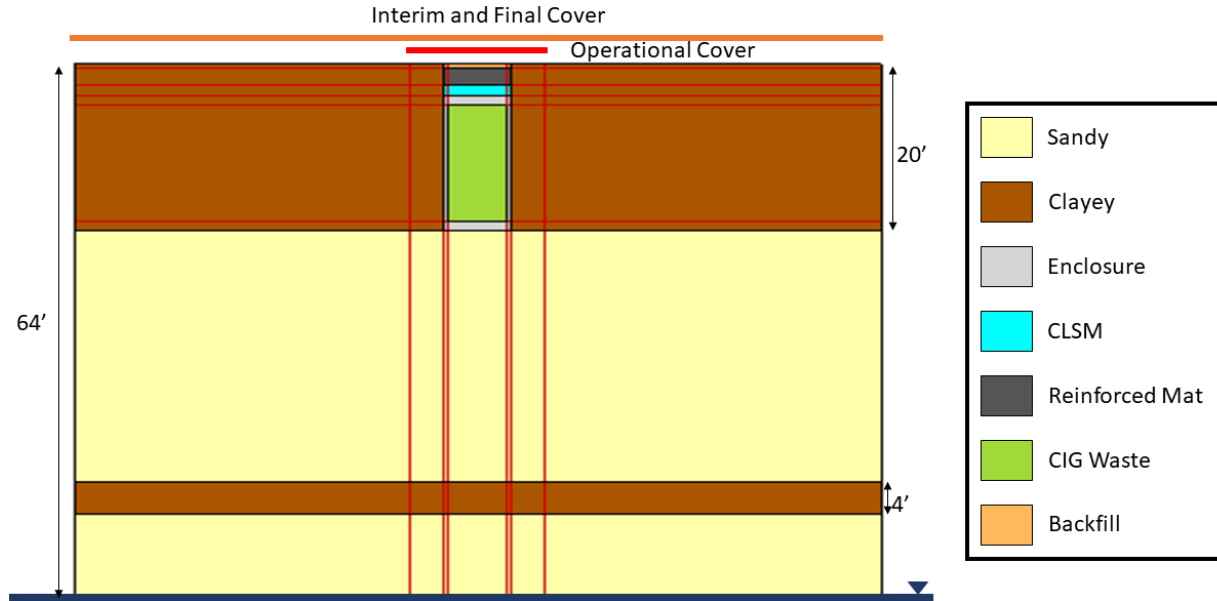


Figure 2-2. Material layout of cross-sectional model of component-in-grout unit.

2.2 Timeline and Boundary Conditions

The timeline of operations and closure serves as the basis for the placement of waste and closure sequencing during simulation of radionuclide transport and for specification of water infiltration boundary conditions. As a conservative assumption, all waste is assumed to be placed at the date of the start of operations for each CIG unit, shown in Table 2-1. The reference date is taken as the start of the ELLWF operations which is assumed to be 9/28/1994, or the start of the Low Activity Waste Vault.

Table 2-1. Date of first waste placement in each component-in-grout unit – relative times are rounded to the nearest integer year.

CIG Segment	Date	Relative Time
CIG 1	8/29/2000	6
CIG 2	7/17/2001	7
CIG 3	7/17/2001	7
CIG 4	8/7/2002	8
CIG 5	9/10/2002	8
CIG 6	8/21/2003	9
CIG 7	8/21/2003	9
CIG 8	8/18/2004	10
CIG 9	6/4/2007	13

Flow fields are computed for pre-determined water infiltration rate boundary conditions out to 1271 years, or 1100 years after the end of institutional control. For each CIG unit, the 1271-year period is discretized into 74 time periods such that steady-state flow fields are computed based on the infiltration transients for conditions representing the operational, operational closure, interim closure, and final closure time periods. Bounding water infiltration rates (Table 2-2) for the intact final closure cap are reported in Dyer (2019) and have been linearly interpolated across the midpoints of the 74 time intervals. The requirement for an operational runoff cover was documented in the current ELLWF closure plan (Phifer et al. 2009) and states that an operational runoff cover should be placed over the CIG segment no more than three months after the placement of the last waste. Given that this conclusion was reached ~2 years after the operational closure of CIG-1 through 8, each of these units is given the same date for the application of the operational runoff cover representing relative year 12 (i.e., 4/1/2006). CIG-9 began operation after this date and therefore its operational cover is placed at relative year 13. The interim and final covers are placed at relative year 46 and 171, respectively.

Table 2-2. Time-dependent water infiltration rate through the intact final closure cap as reported in Dyer (2019).

Relative Year	Intact
<i>No Cover</i>	15.78
<i>Operational Cover</i>	0.1
46	0.1
171	0.0008
251	0.0070
361	0.16
371	0.18
411	0.30
451	0.38
551	1.39
731	3.23
1171	6.82
1971	10.24
2794	11.10
3371	11.18
5771	11.30
10171	11.35

In addition to the intact infiltration conditions, four CIG units, CIG-4 through CIG-7, contain components or low-density waste that are not filled with grout and have been estimated to have a maximum of 7 feet of subsidence potential (Nichols and Butcher 2020). In the conceptual model implementation, subsidence is assumed to occur only over the waste zone (i.e., excluding the grout encapsulation along the walls of the trench segment) where settling and degradation of the composite cementitious waste form occurs. Two cases have been considered: a bounding case, where subsidence occurs immediately at final closure, and a best estimate case, where subsidence occurs 200 years after the end of institutional control. The latter is based on the work of Peregoy (2006), Jones et al (2004), and Phifer (2004) who explored the subsidence potential of the waste in each segment. Subsided infiltration rates are based on the formulation presented by Dyer (2019) to account for the background rainfall minus evapotranspiration and the upslope intact area expressed as:

$$I_S = I_B + \frac{L_U}{L_H} (I_B - I_I)$$

where, I_B is the background rainfall minus evapotranspiration, 16.5 inches/year, L_U is the length of the upslope intact area, L_H is the length of the subsided region (i.e., the length of the grouted component), and I_I is the intact infiltration rate at a given time. Table 2-3 provides the bounding and best estimate infiltration cases for CIG 4 through 7. The as-built layout of the CIG units is shown in Figure 2-3. The dimensions of each CIG unit have been used to compute the length of the subsided region and the upslope intact distance between the crest of the final closure cap (located approximately 110 feet from the edge of the ST nearest CIG-1 and CIG-7) and the edge of the unit closest to the crest. The upslope intact length and subsided region lengths used for calculating subsided infiltration rates for CIG-4 through CIG-7 are shown in Table 2-4.

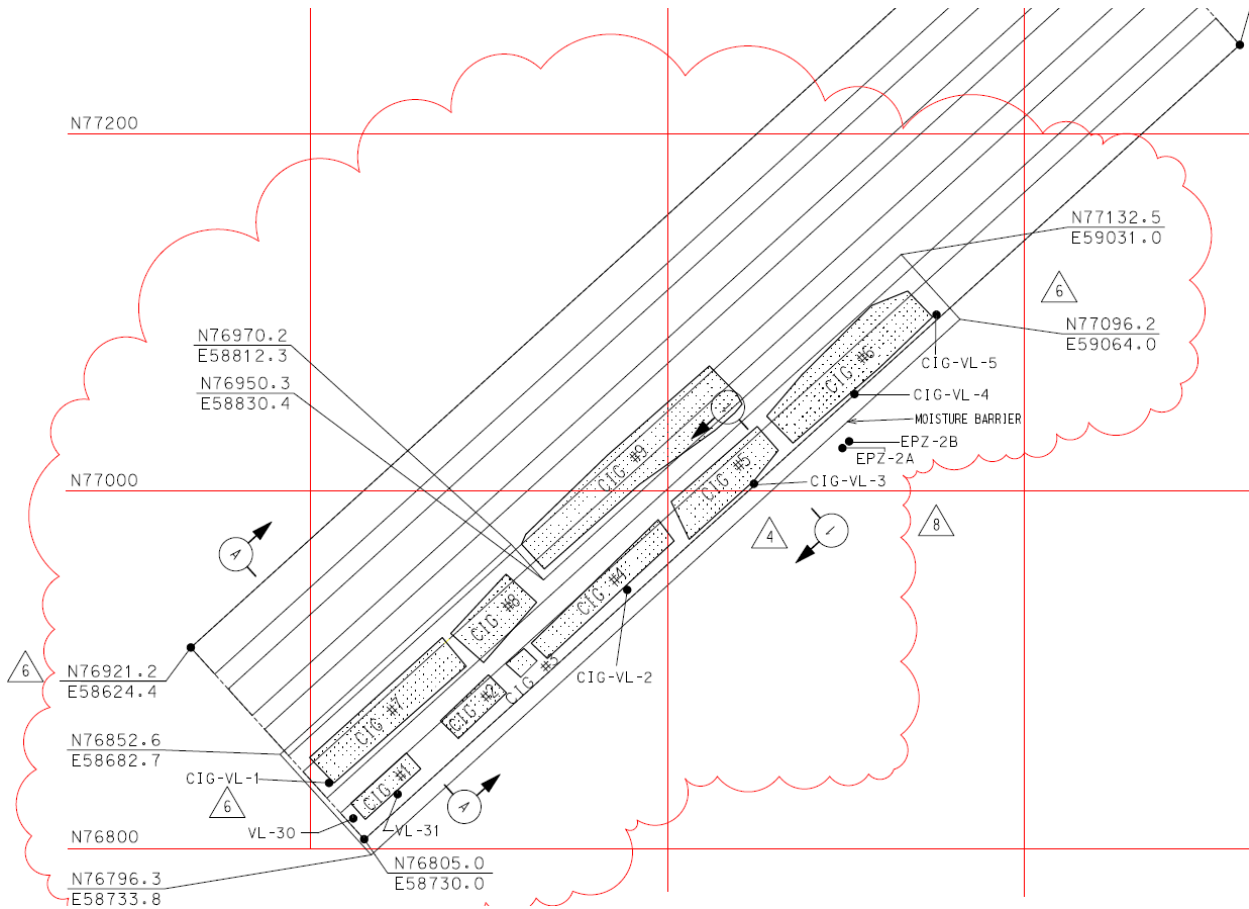


Figure 2-3. Layout of as-built component-in-grout units 1 through 9 within the ST 23 footprint.

Table 2-3. Infiltration rates in inches/year for the bounding and best estimate cases for CIG-4 through -7.

Relative Year	Intact	Bounding Case				Best Estimate Case			
		CIG-4	CIG-5	CIG-6	CIG-7	CIG-4	CIG-5	CIG-6	CIG-7
<i>No Cover</i>	15.78	15.78	15.78	15.78	15.78	15.78	15.78	15.78	15.78
<i>Operational Cover</i>	0.1	0.10	0.10	0.10	0.10	0.10	0.10	0.10	0.10
46	0.1	0.10	0.10	0.10	0.10	0.10	0.10	0.10	0.10
171	0.0008	33.43	55.57	62.86	16.82	0.00	0.00	0.00	0.00
251	0.0070	33.43	55.56	62.84	16.82	0.01	0.01	0.01	0.01
361	0.16	33.27	55.20	62.41	16.82	0.16	0.16	0.16	0.16
371	0.18	33.25	55.15	62.35	16.82	33.25	55.15	62.35	16.82
411	0.30	33.13	54.86	62.02	16.82	33.13	54.86	62.02	16.82
451	0.38	33.04	54.68	61.79	16.82	33.04	54.68	61.79	16.82
551	1.39	32.01	52.28	58.95	16.80	32.01	52.28	58.95	16.80
731	3.23	30.12	47.93	53.78	16.76	30.12	47.93	53.78	16.76
1171	6.82	26.44	39.42	43.70	16.69	26.44	39.42	43.70	16.69
1971	10.24	22.92	31.32	34.09	16.62	22.92	31.32	34.09	16.62
2794	11.10	22.04	29.29	31.67	16.61	22.04	29.29	31.67	16.61
3371	11.18	21.96	29.10	31.45	16.60	21.96	29.10	31.45	16.60
5771	11.30	21.84	28.81	31.11	16.60	21.84	28.81	31.11	16.60
10171	11.35	21.79	28.70	30.97	16.60	21.79	28.70	30.97	16.60

Table 2-4. Upslope intact length and subsided region lengths used for calculating subsided infiltration rates.

CIG Unit	Upslope distances (ft)	Segment Lengths (ft)
<i>CIG-4</i>	33.1	32.25
<i>CIG-5</i>	144.46	61
<i>CIG-6</i>	216.34	77
<i>CIG-7</i>	1.67	85

2.3 Physical and Chemical Properties

The specific values of the physical and chemical properties of the composite cementitious waste form and the surrounding native soils of the upper and lower vadose zone are discussed in the SRNL Hydraulic Properties Data Package (Nichols and Butcher, 2020) and the SRNL Geochemical Data Package (Kaplan, 2016). As water passes through the CIG wastefrom, chemical constituents are leached from the cementitious materials which leads to a gradual physical degradation and a decrease in the hydraulic integrity (i.e., increased porosity and hydraulic conductivity). The physical degradation of the cementitious materials is represented by step-changes at pre-determined times corresponding to the operational, interim closure, and final closure time periods. Most notably, the CIG degrades from an intact CIG wastefrom to the degraded wastefrom at simulation time 40 years, where the hydraulic conductivity increases by nine orders of magnitude. At 371 years (i.e., 200 years after the end of institutional control), the CIG wastefrom is considered fully degraded. The material types and the values of the physical properties assigned to each

material zone (Figure 2-2) are shown in Table 2-5 and Table 2-6. Note that dynamic compaction is not performed over CIG waste.

Table 2-5. Material types applied to each material zone through time.

Material Type	Time Interval	CIG 1 through CIG 7	CIG 8	CIG 9
Backfill	0 - 40	OSC Before	OSC Before	OSC Before
	40 - 171	OSC Before	OSC Before	OSC Before
	171 - 371	OSC Before	OSC Before	OSC Before
	371+	OSC Before	OSC Before	OSC Before
Reinforced Mat	0 - 40	OSC Before	EareaConcreteMats	EareaConcreteMats
	40 - 171	OSC Before	EareaConcreteMats	EareaConcreteMats
	171 - 371	OSC Before	EareaConcreteMats	EareaConcreteMats
	371+	OSC Before	OSC Before	OSC Before
CLSM	0 - 40	OSC Before	CLSM	CLSM
	40 - 171	OSC Before	CLSM	CLSM
	171 - 371	OSC Before	CLSM	CLSM
	371+	OSC Before	OscBefore	OscBefore
Enclosure	0 - 40	CIGgrout1to8	CIGgrout1to8	CIGgrout9on
	40 - 171	CIGgrout1to8	CIGgrout1to8	CIGgrout9on
	171 - 371	CIGgrout1to8	CIGgrout1to8	CIGgrout9on
	371+	OscBefore	OscBefore	OscBefore
CIG Waste	0 - 40	CIGint	CIGint	CIGint
	40 - 171	CIGdeg	CIGdeg	CIGdeg
	171 - 371	CIGdeg	CIGdeg	CIGdeg
	371+	CIGdeg	CIGdeg	CIGdeg
Sandy	All	LowerVadoseZone	LowerVadoseZone	LowerVadoseZone
Clayey	All	UpperVadoseZone	UpperVadoseZone	UpperVadoseZone

Table 2-6. Physical properties for each material type.

Material Type	Kh (cm/yr)	Kv (cm/yr)	De (cm ² /yr)	Porosity	Bulk Density (g/cm ³)
<i>OSC Before</i>	4.10E+03	4.10E+03	1.67E+02	0.456	1.44
<i>CIGgrout1to8</i>	1.42E+03	1.42E+03	6.00E+01	0.224	1.79
<i>CIGgrout9on</i>	2.84E+01	2.84E+01	2.52E+01	0.233	1.90
<i>CLSM</i>	6.94E+01	6.94E+01	1.26E+02	0.328	1.78
<i>CIGdeg</i>	3.16E-05	3.16E-05	1.67E+02	0.456	1.44
<i>CIGint</i>	3.79E+03	3.79E+03	1.67E+02	0.456	1.44
<i>EareaConcreteMats</i>	2.84E-01	2.84E-01	2.52E+01	0.233	1.90
<i>UpperVadoseZone</i>	1.96E+03	2.75E+02	1.67E+02	0.385	1.65
<i>LowerVadoseZone</i>	1.04E+04	2.87E+03	1.67E+02	0.380	1.66

In addition to degradation of physical properties, as chemical constituents are leached from cementitious material zones, chemical degradation occurs leading to a reduction in the partition coefficient (i.e., K_d) of radionuclide contaminants. The degradation of cementitious materials occurs across four stages from young (Stage I) to old (Stage III) and is tracked through time based on the number of pore volumes of water that have passed through the material. Past Stage III, the enhanced chemical attenuation of the cementitious materials is assumed to be gone and the K_d returns to that of the surrounding soils. The cementitious aging occurs as follows:

- Stage I (“Young”) – 0 to 50 pore volumes
- Stage II (“Middle”) – 50 to 500 pore volumes
- Stage III (“Old”) – 500 to 7,000 pore volumes
- Beyond (“Gone”) – greater than 7,000 pore volumes

The reduction in K_d at each stage occurs in a stepwise fashion, where a post-processing algorithm computes the number of pore volumes through each cementitious material zone for the specific CIG unit during each of the 74 time intervals. Because flow occurs in both the x and y directions of the 2D simulations and steady-state flow fields are supplied to transport such that there is a fixed saturation profile across the entire mesh at time 0, all cementitious materials are considered to be chemically aged simultaneously rather than sequentially. The latter approach would delay the chemical aging process and slow the release of radionuclide contaminants further out in time and therefore, the simultaneous aging approach is considered to be conservative. For each cementitious zone, the number of pore volumes per unit time is computed using the expression:

$$\Phi_i(t) = \frac{Q_i(t)}{V_i(t)}$$

Where, Φ_i - Number of pore volume flushes through i^{th} material zone per time (# PVs/yr)
 Q_i - Volumetric flowrate passing through the i^{th} material zone volume (ml/yr)
 V_i - Total pore volume of i^{th} material zone (void space available for water) (ml)

By computing Φ_i , the transition time between stages for each cementitious material zone can be computed over the course of the CIG timeline by dividing the number of pore volumes to transition by Φ_i .

As chemical constituents are leached from the cementitious materials above the lower vadose zone, the K_d within the neighboring soils is multiplied by a cementitious leachate factor until all cementitious regions have been fully chemically depleted. During the implementation of the conceptual model, an abbreviated

suite of seven parent radionuclides has been tested. The K_d 's and half-lives are shown for each is shown in Table 2-7.

Table 2-7. Half-lives and K_d 's for the suite of radionuclides tested during implementation. Parent radionuclides are in bold and progeny are not bold.

Species	Half-Life (years)	Stage I (mL/g)	Stage II (mL/g)	Stage III (mL/g)	Gone (mL/g)	Cementitious Leachate Factor	Sandy (mL/g)	Clayey (mL/g)
C-14	5.70E+03	2000	5000	50	30	5	1	30
H-3	1.23E+01	0	0	0	0	1	0	0
I-129	1.57E+07	8	10	4	3	0.1	1	3
Np-237	2.14E+06	10000	10000	5000	9	1.5	3	9
U-233	1.59E+05	1000	5000	5000	400	3	300	400
Th-229	7.34E+03	10000	10000	2000	2000	2	900	2000
Sr-90	2.88E+01	90	15	90	17	3	5	17
Tc-99	2.11E+05	0.8	0.8	0.5	1.8	0.1	0.6	1.8
U-238	4.47E+09	1000	5000	5000	400	3	300	400
U-234	2.46E+05	1000	5000	5000	400	3	300	400
Th-230	7.54E+04	10000	10000	2000	2000	2	900	2000
Ra-226	1.60E+03	200	100	200	180	3	25	180
Pb-210	2.22E+01	300	300	100	5000	3.2	2000	5000

3.0 Results and Discussion

In the current section, preliminary results are presented to demonstrate that the pre- and post-processing automation schemes and the conceptual approach are implemented correctly. Prior to the final runs for the PA, all parameters will be updated to reflect the most up-to-date values. The temporal discretization into 74 time periods is listed in Table 3-1, where a steady-state flow field is computed for each time interval which serves as input to radionuclide transport simulations.

Table 3-1. Temporal discretization of the performance assessment time period. First waste and the time to the operation cover are CIG-unit dependent (reference Section 2.2).

Time Period	Start Year	End Year
<i>TI01</i>	0.00	First Waste
<i>TI02</i>	First Waste	Operational Cover
<i>TI03</i>	Operational Cover	46.00
<i>TI04</i>	46.00	171.00
<i>TI05</i>	171.00	181.00
<i>TI06</i>	181.00	191.00
<i>TI07</i>	191.00	201.00
<i>TI08</i>	201.00	211.00
<i>TI09</i>	211.00	221.00
<i>TI10</i>	221.00	231.00
<i>TI11</i>	231.00	241.00
<i>TI12</i>	241.00	251.00
<i>TI13</i>	251.00	261.00

<i>TI14</i>	261.00	271.00
<i>TI15</i>	271.00	281.00
<i>TI16</i>	281.00	291.00
<i>TI17</i>	291.00	301.00
<i>TI18</i>	301.00	311.00
<i>TI19</i>	311.00	321.00
<i>TI20</i>	321.00	331.00
<i>TI21</i>	331.00	341.00
<i>TI22</i>	341.00	351.00
<i>TI23</i>	351.00	361.00
<i>TI24</i>	361.00	371.00
<i>TI25</i>	371.00	381.00
<i>TI26</i>	381.00	391.00
<i>TI27</i>	391.00	401.00
<i>TI28</i>	401.00	411.00
<i>TI29</i>	411.00	421.00
<i>TI30</i>	421.00	431.00
<i>TI31</i>	431.00	441.00
<i>TI32</i>	441.00	451.00
<i>TI33</i>	451.00	461.00
<i>TI34</i>	461.00	471.00
<i>TI35</i>	471.00	481.00
<i>TI36</i>	481.00	491.00
<i>TI37</i>	491.00	501.00
<i>TI38</i>	501.00	511.00
<i>TI39</i>	511.00	521.00
<i>TI40</i>	521.00	531.00
<i>TI41</i>	531.00	541.00
<i>TI42</i>	541.00	561.00
<i>TI43</i>	561.00	581.00
<i>TI44</i>	581.00	601.00
<i>TI45</i>	601.00	621.00
<i>TI46</i>	621.00	641.00
<i>TI47</i>	641.00	661.00
<i>TI48</i>	661.00	681.00
<i>TI49</i>	681.00	701.00
<i>TI50</i>	701.00	721.00
<i>TI51</i>	721.00	741.00
<i>TI52</i>	741.00	761.00
<i>TI53</i>	761.00	781.00
<i>TI54</i>	781.00	801.00
<i>TI55</i>	801.00	821.00
<i>TI56</i>	821.00	841.00
<i>TI57</i>	841.00	861.00
<i>TI58</i>	861.00	881.00
<i>TI59</i>	881.00	901.00
<i>TI60</i>	901.00	921.00

<i>TI61</i>	921.00	941.00
<i>TI62</i>	941.00	961.00
<i>TI63</i>	961.00	981.00
<i>TI64</i>	981.00	1001.00
<i>TI65</i>	1001.00	1021.00
<i>TI66</i>	1021.00	1041.00
<i>TI67</i>	1041.00	1061.00
<i>TI68</i>	1061.00	1081.00
<i>TI69</i>	1081.00	1101.00
<i>TI70</i>	1101.00	1121.00
<i>TI71</i>	1121.00	1141.00
<i>TI72</i>	1141.00	1161.00
<i>TI73</i>	1161.00	1211.00
<i>TI74</i>	1211.00	1261.00

3.1 Preliminary Flow Results

The saturation profiles for CIG-4, which are representative of CIG-1 through CIG-7, are shown in Figure 3-1 through Figure 3-6 for the intact conditions through 371 years. Notably, the majority of the rainfall that infiltrates from the top boundary is redirected laterally around the cementitious waste form and its outer enclosure prior to hydraulic degradation in the first 40 years. After hydraulic degradation of the low permeability CIG waste, the water passing through the cementitious mass increases, though the velocity is low due to the high integrity closure cap systems. As the cap degrades, the water velocity through the CIG increases.

Saturation profiles for CIG-8 and CIG-9 are shown in Figure 3-7 through Figure 3-18 out to 371 years to display the impact of the reinforced concrete mat on the flow field and also the improved grout formulation that was used for disposal in CIG-9. In a similar manner to CIG-1 through CIG-7, most of the water is redirected laterally around the CIG mass, however, the water velocity is substantially decreased in the regions above the waste zone due to the reinforced concrete mats, which results in a higher water saturation above the waste zone. After hydraulic degradation of the CIG waste zone, the hydraulic properties of the reinforced concrete mat do not lead to any increased redirection of water around the CIG mass, demonstrating they are primarily for structural integrity.

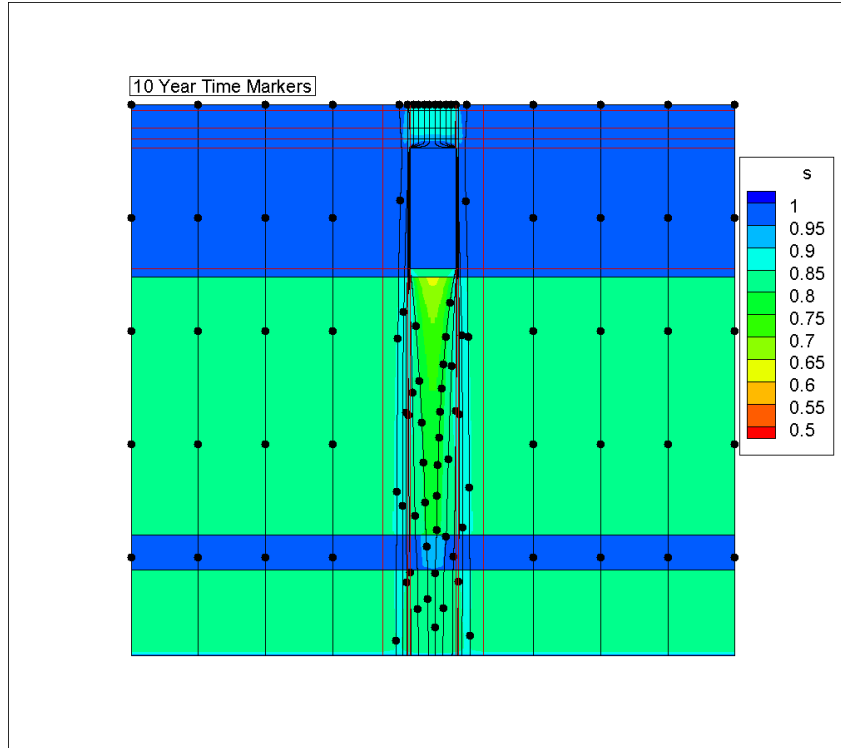


Figure 3-1. Saturation profile for CIG-4 during the operational period.

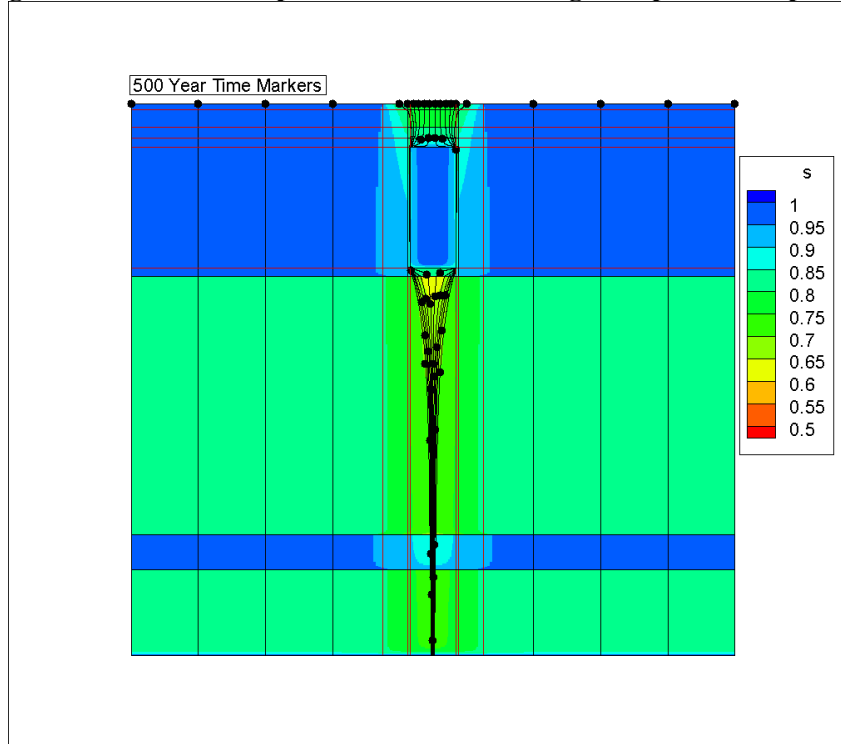


Figure 3-2. Saturation profile for CIG-4 during the operational closure period.

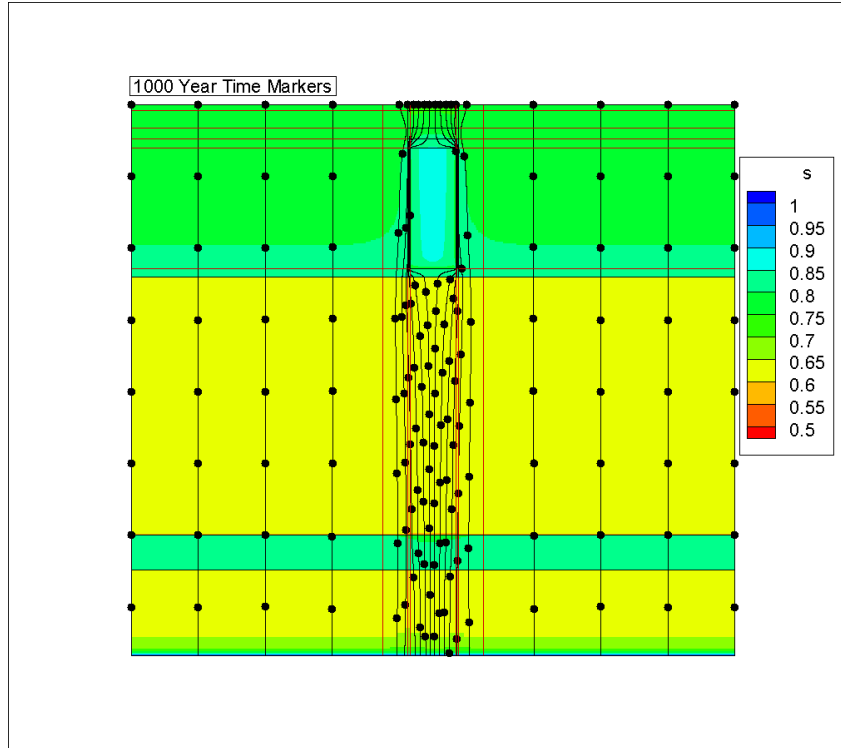


Figure 3-3. Saturation profile for CIG-4 during the interim closure period, prior to hydraulic degradation.

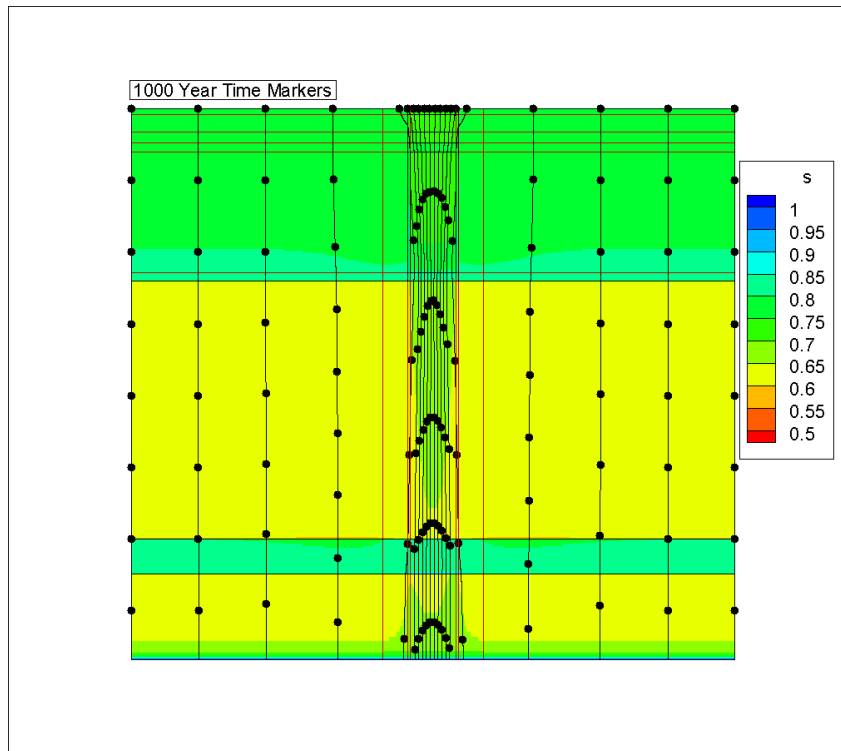


Figure 3-4. Saturation profile for CIG-4 during the interim closure period, after hydraulic degradation.

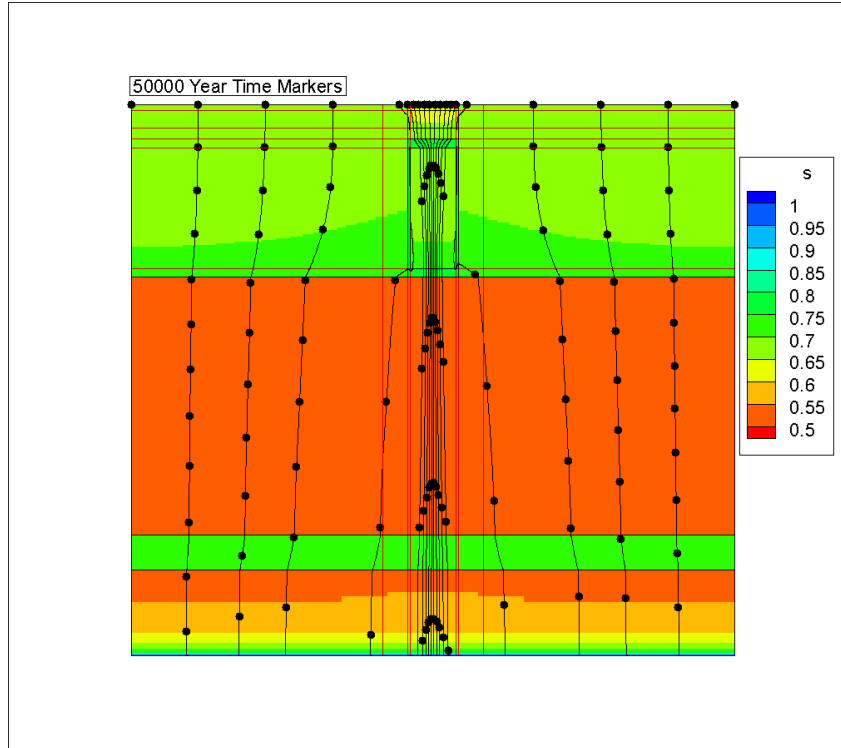


Figure 3-5. Saturation profile for CIG-4 at the end of institutional control.

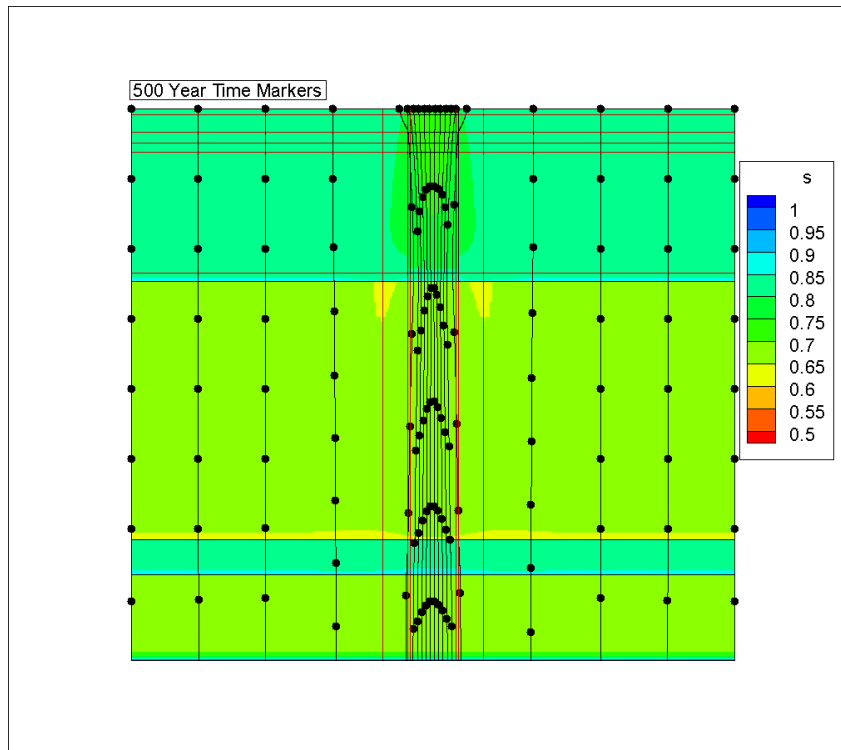


Figure 3-6. Saturation profile for CIG-4 at 371 years.

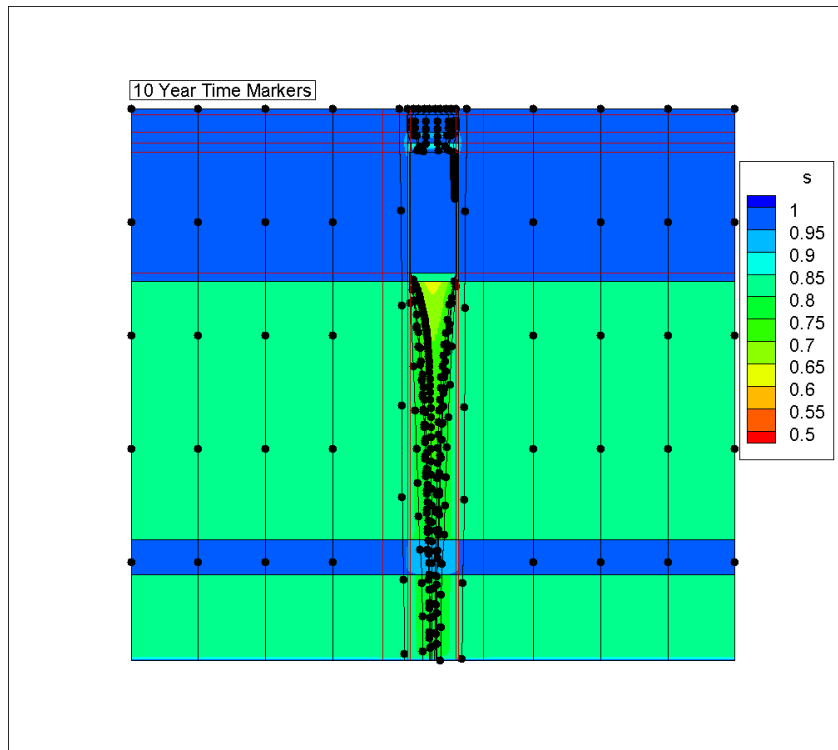


Figure 3-7. Saturation profile for CIG-8 during the operational time period.

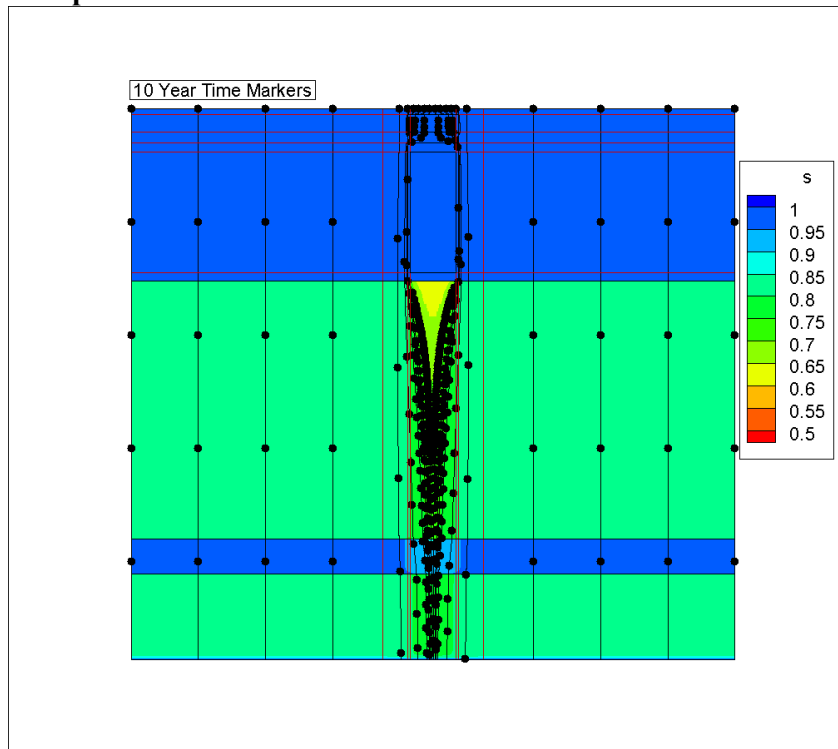


Figure 3-8. Saturation profile for CIG-9 during the operational time period.

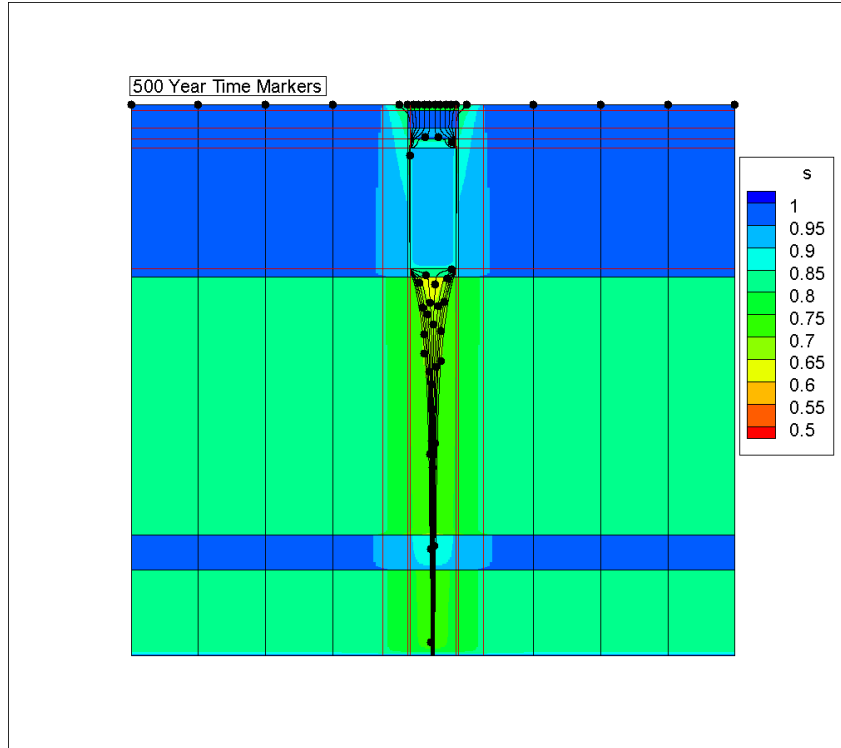


Figure 3-9. Saturation profile for CIG-8 during the operational closure period.

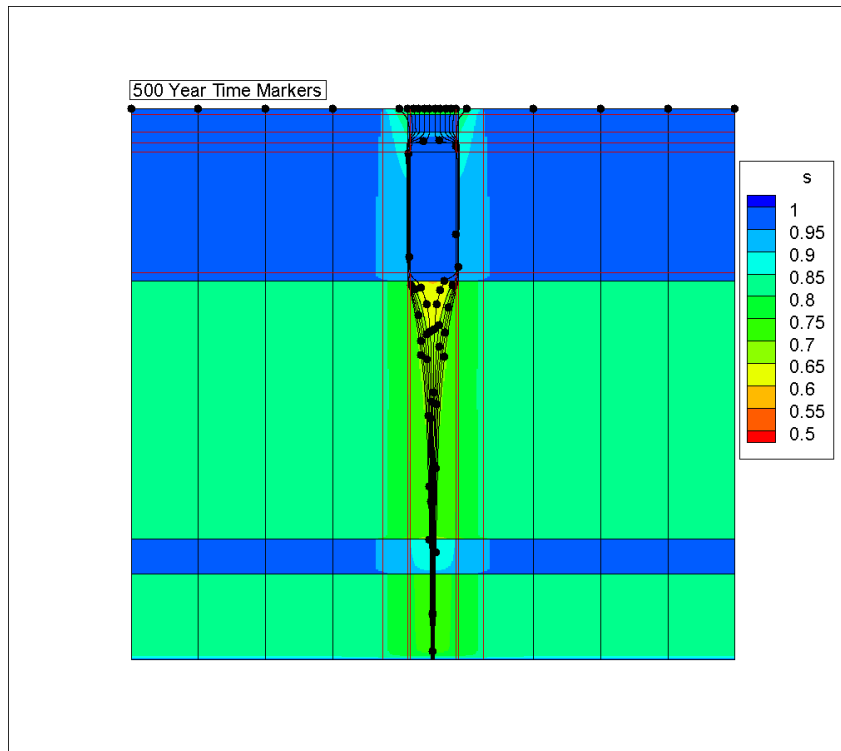


Figure 3-10. Saturation profile for CIG-9 during the operational closure period.

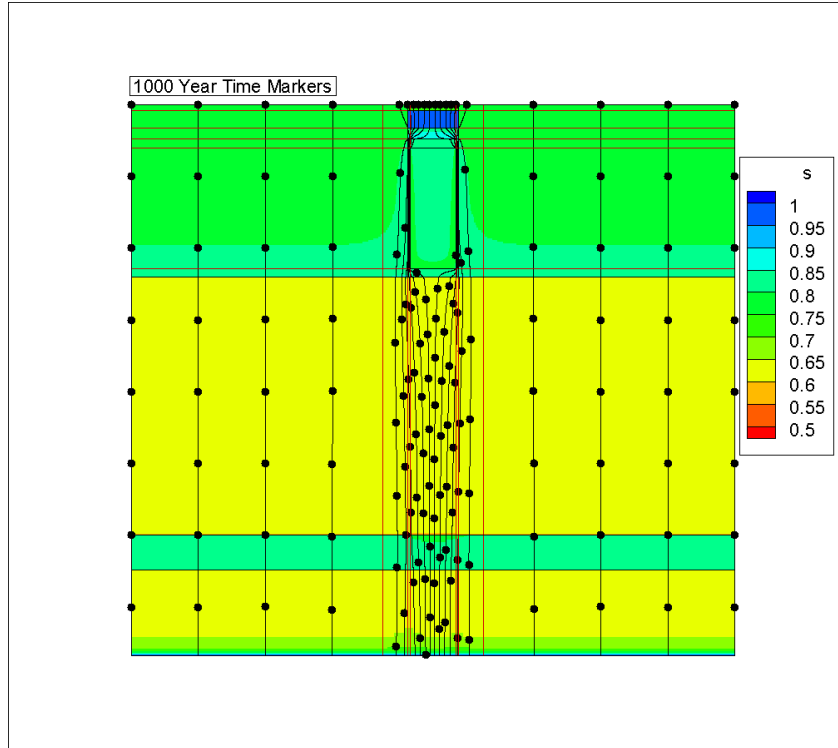


Figure 3-11. Saturation profile for CIG-8 during the interim closure period, prior to hydraulic degradation.

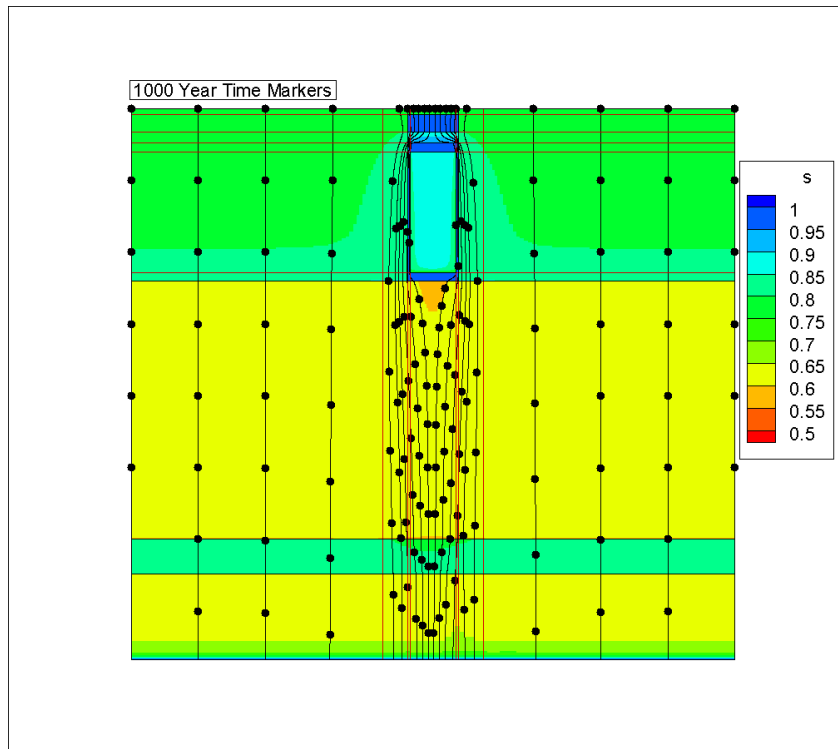


Figure 3-12. Saturation profile for CIG-9 during the interim closure period, prior to hydraulic degradation.

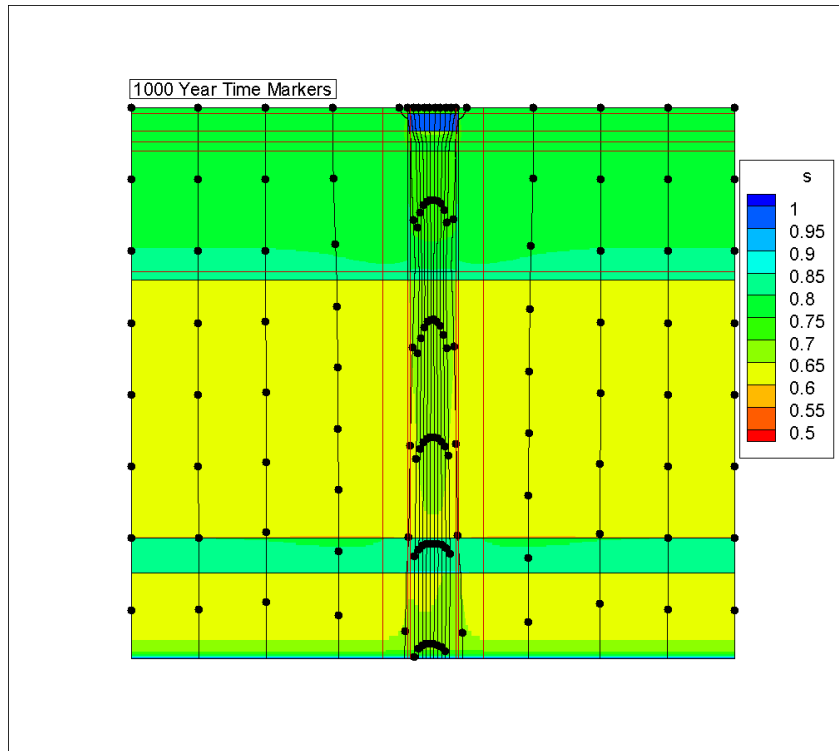


Figure 3-13. Saturation profile for CIG-8 during the interim closure period, after hydraulic degradation.

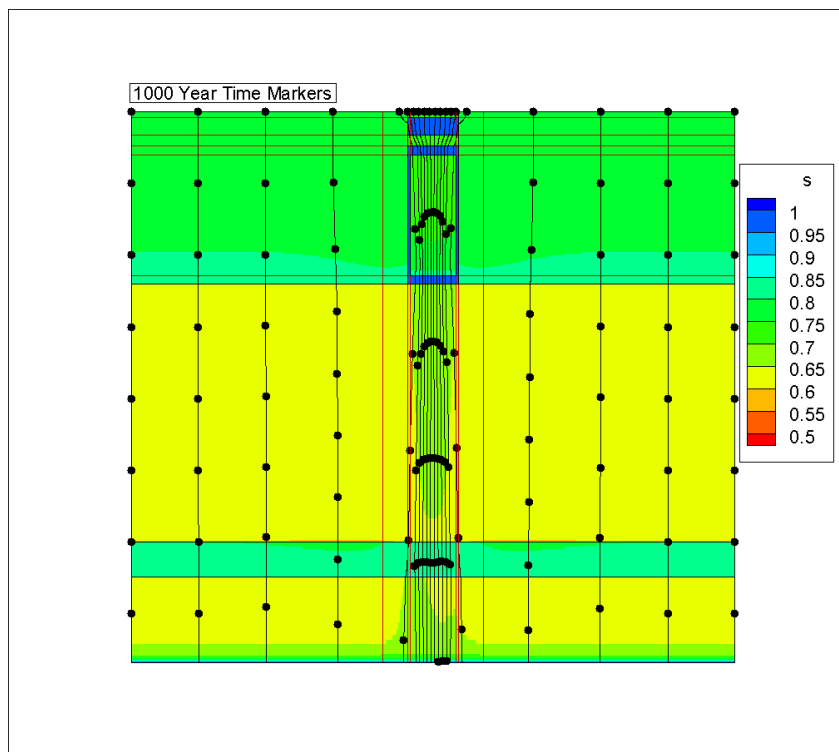


Figure 3-14. Saturation profile for CIG-9 during the interim closure period, after hydraulic degradation.

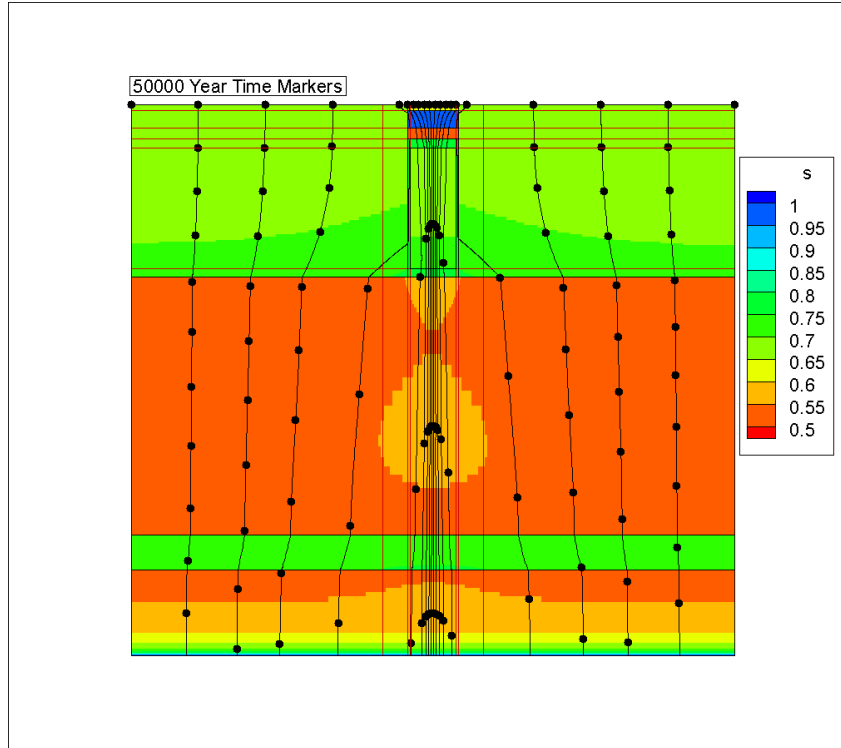


Figure 3-15. Saturation profile for CIG-8 at the end of institutional control.

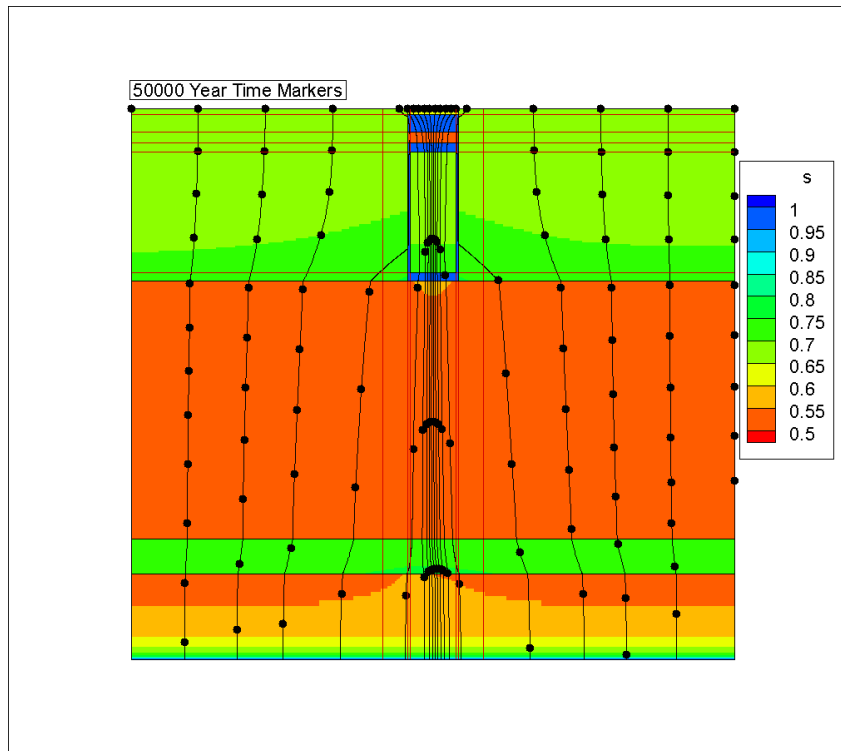


Figure 3-16. Saturation profile for CIG-9 at the end of institutional control.

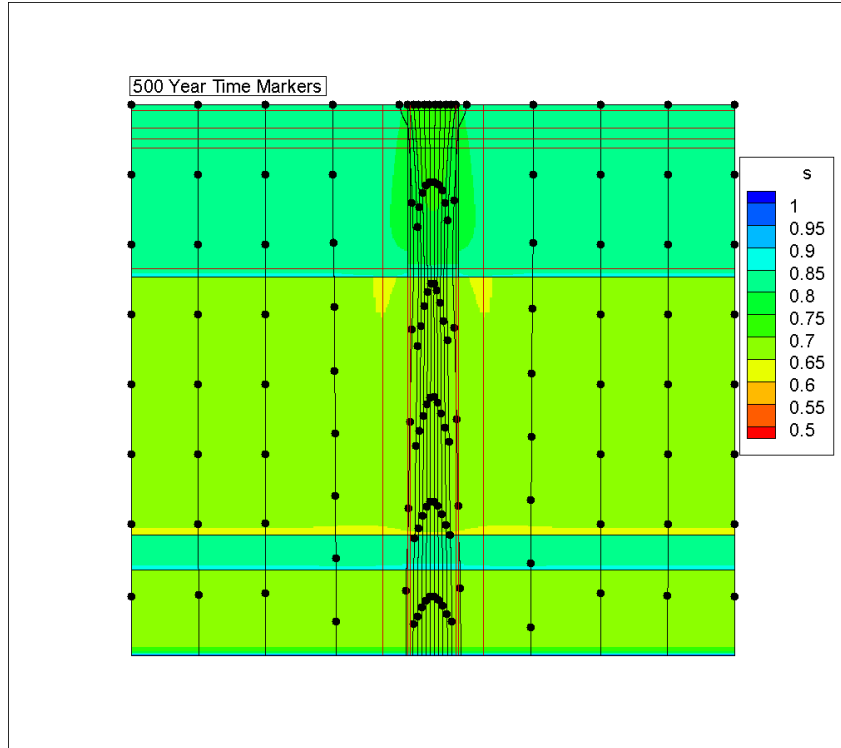


Figure 3-17. Saturation profile for CIG-8 at 371 years.

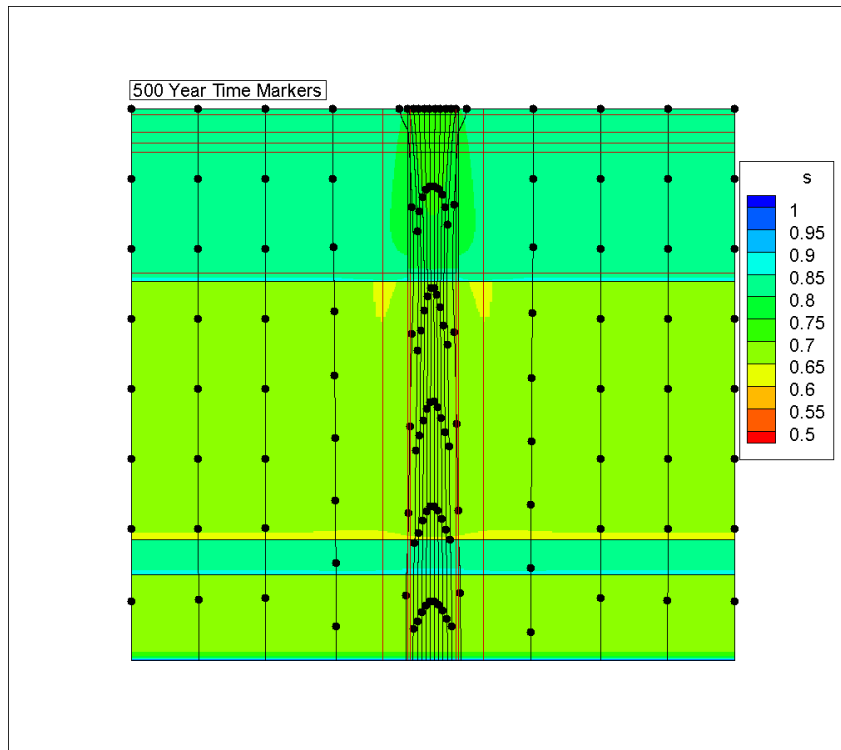


Figure 3-18. Saturation profile for CIG-9 at 371 years.

The saturation profiles for the CIG-4 bounding and best estimate subsidence cases are shown in Figure 3-19 and Figure 3-20. Notably, subsidence in the bounding case occurs immediately upon final closure. Meanwhile, the lateral extent of the final closure cap is essentially undegraded outside the subsided region which allows for lateral spreading as water infiltrates through the subsided region. In contrast, subsidence in the best estimate case occurs at 371 years (i.e., 200 years after the end of institutional control), where the final closure cap has undergone more degradation and produces significantly reduced lateral spreading of infiltrating water and a more uniform saturation profile. The water velocity through the subsided region, however, does not differ substantially, as shown in Table 2-3.

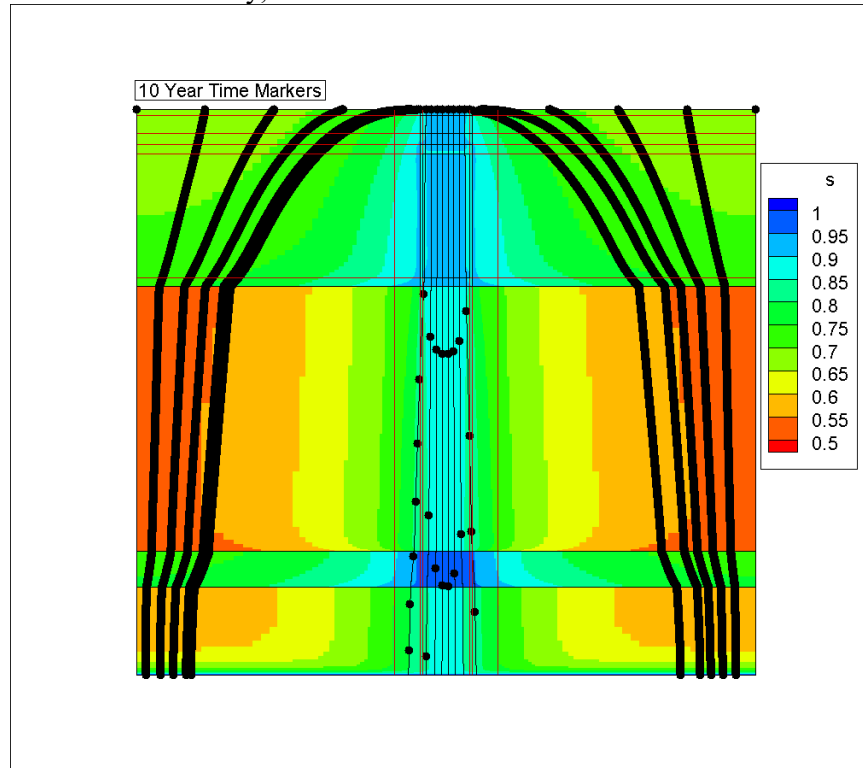


Figure 3-19. Saturation profile for CIG-4 with subsidence at 171 years.

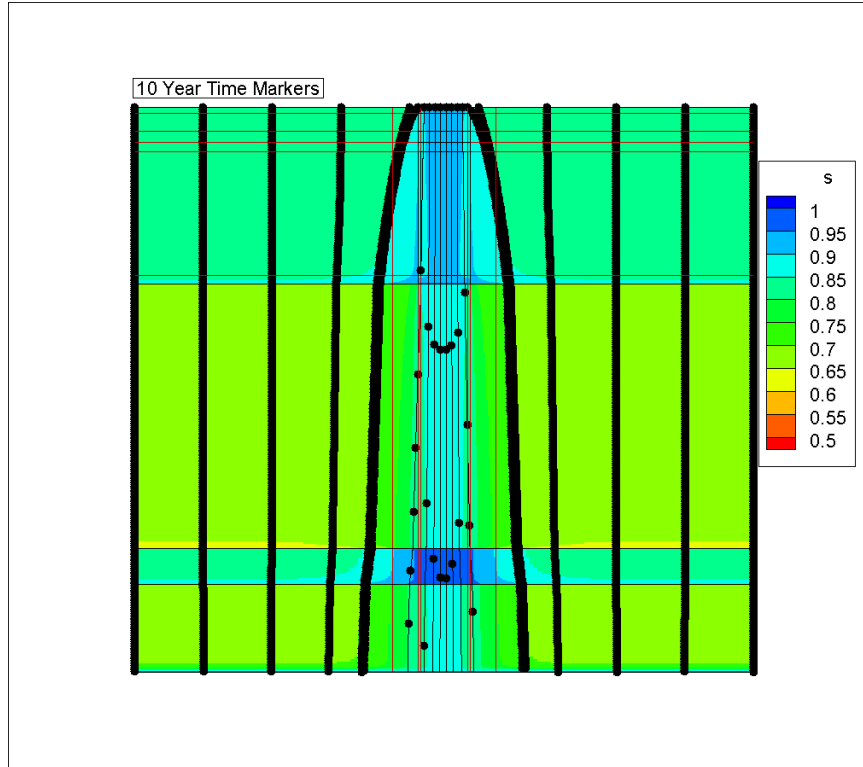


Figure 3-20. Saturation profile for CIG-4 with subsidence at 371 years.

3.2 Preliminary Transport Results

The aging times for each cementitious material region are shown in Table 3-2 for CIG units 4, 8, and 9 and have been computed using the steady-state flow fields for each time interval and each CIG unit. These aging times serve as triggers for making stepwise changes to the partition coefficient of each radionuclide species during PORFLOW transport simulations. The bounding subsidence case for CIG-4 has the shortest cementitious aging times resulting from the elevated water infiltration in the subsided time periods which first occur at the end of institutional control. The best estimate subsided case for CIG-4 has the second fastest aging times. Neither the presence of the reinforced concrete mats in CIG-8 and 9 nor the improved grout formulation (i.e., lower hydraulic conductivity) used in CIG-9 substantially increase aging times as the early transition from Stage I to Stage II occurs after the degradation of these features. Notably, none of the CIG units ever reach the full chemical aging during the 1271-year simulation time.

Table 3-2. Cementitious material aging times (simulation year referenced from the start of operations in the ELLWF) computed from the steady-state flow fields.

Unit	Case	Transition	Enclosure	CIG	Reinforced Mat	CLSM
CIG-4	Intact	Stage I to Stage II	622	1157	-	-
		Stage II to Stage III	1288	4716	-	-
		Stage III to Stage IV	8172	56099	-	-
CIG-4	Bounding Subsidence	Stage I to Stage II	177	297	-	-
		Stage II to Stage III	251	1551	-	-
		Stage III to Stage IV	2484	20521	-	-
CIG-4	Best Estimate Subsidence	Stage I to Stage II	328	497	-	-
		Stage II to Stage III	524	1775	-	-
		Stage III to Stage IV	2929	20745	-	-
CIG-8	Intact	Stage I to Stage II	636	1157	678	612
		Stage II to Stage III	1292	4716	1423	1189
		Stage III to Stage IV	8176	56099	9948	6674
CIG-9	Intact	Stage I to Stage II	646	1158	680	621
		Stage II to Stage III	1295	4697	1423	1191
		Stage III to Stage IV	8140	55794	9898	6645

Radionuclide transport from the CIG units through the vadose zone has been simulated for a suite of seven parent radionuclides (shown in bold in Table 2-7) to produce a flux to the water table profile. At the start of the CIG unit's operations, 1 gram-mole of inventory is distributed uniformly throughout the 'CIG Waste' material zone (reference Figure 2-2). For those units where subsidence occurs (i.e., CIG-4 through CIG-7), all radionuclide inventory that has not migrated from the waste zone is transferred to the lower half (i.e., the lower 7 feet) of the 'CIG Waste' material zone at the time of subsidence. The flux to the water table profiles for the intact and subsided cases representing CIG-4 are shown in Figure 3-21 through Figure 3-27. Notably, when subsidence occurs later in time, the flux to the water table profile is shifted along the time axis primarily as a result of the difference in the water velocity through the waste zone.

A comparison of the flux to the water table profiles for CIG-4, 8, and 9 are shown in Figure 3-28 through Figure 3-33 for all parent radionuclides with the exception of U-238 (due to the low concentration reaching the water table). The radionuclide flux in the early time periods is lower for CIG-8 and CIG-9 than for CIG-4. This is primarily attributed to the presence of the reinforced concrete mats and the lower hydraulic conductivity of the grout formulation used in CIG-9. Notably, the peak fluxes for the three CIG units are comparable for all radionuclides except for H-3, whose peak occurs prior to complete hydraulic degradation at 371 years.

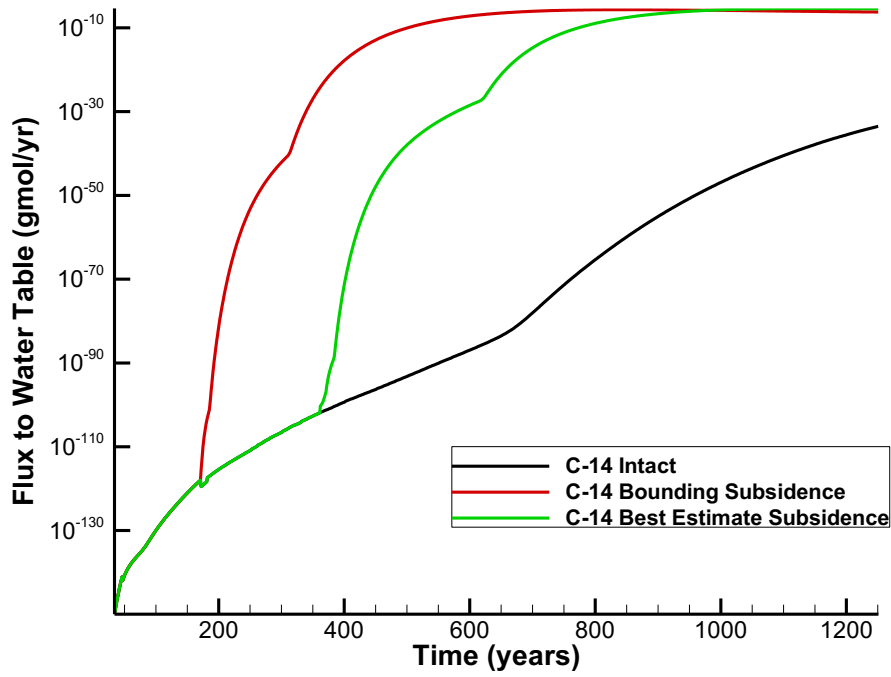


Figure 3-21. C-14 flux to the water table from CIG-4.

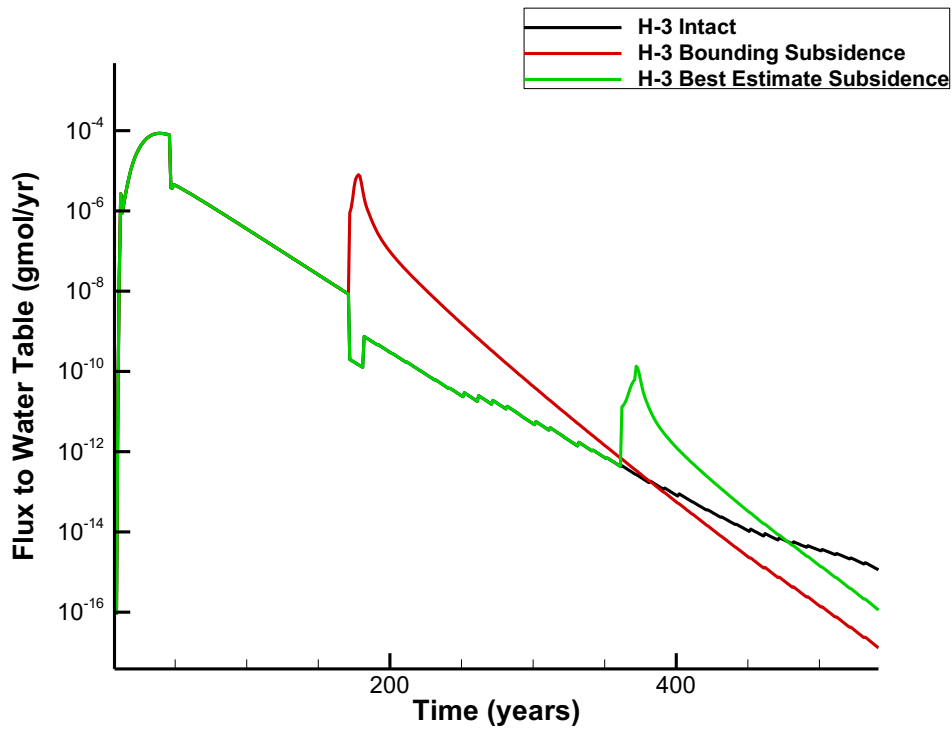


Figure 3-22. H-3 flux to the water table from CIG-4.

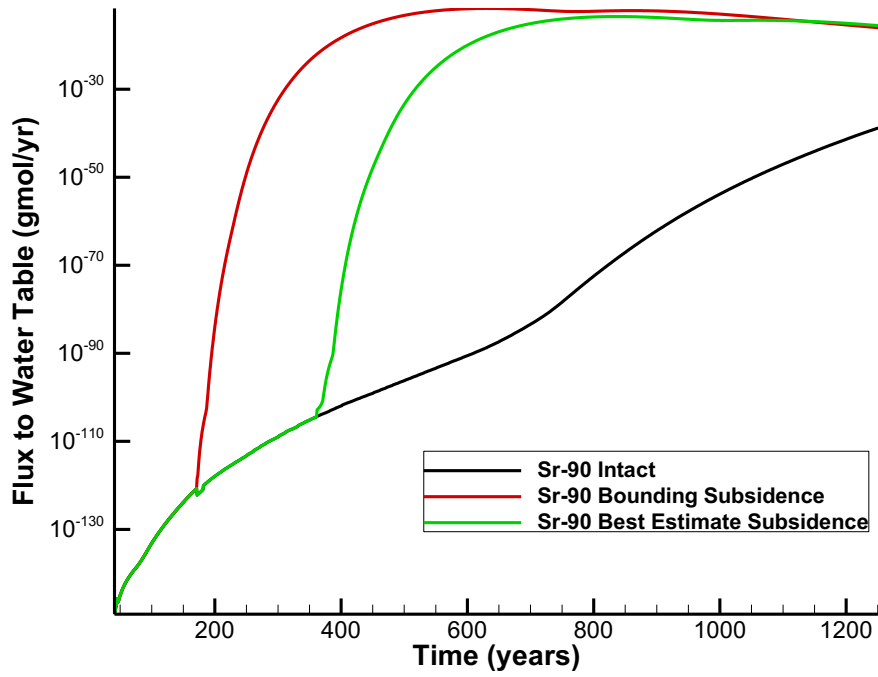


Figure 3-23. Sr-90 flux to the water table from CIG-4.

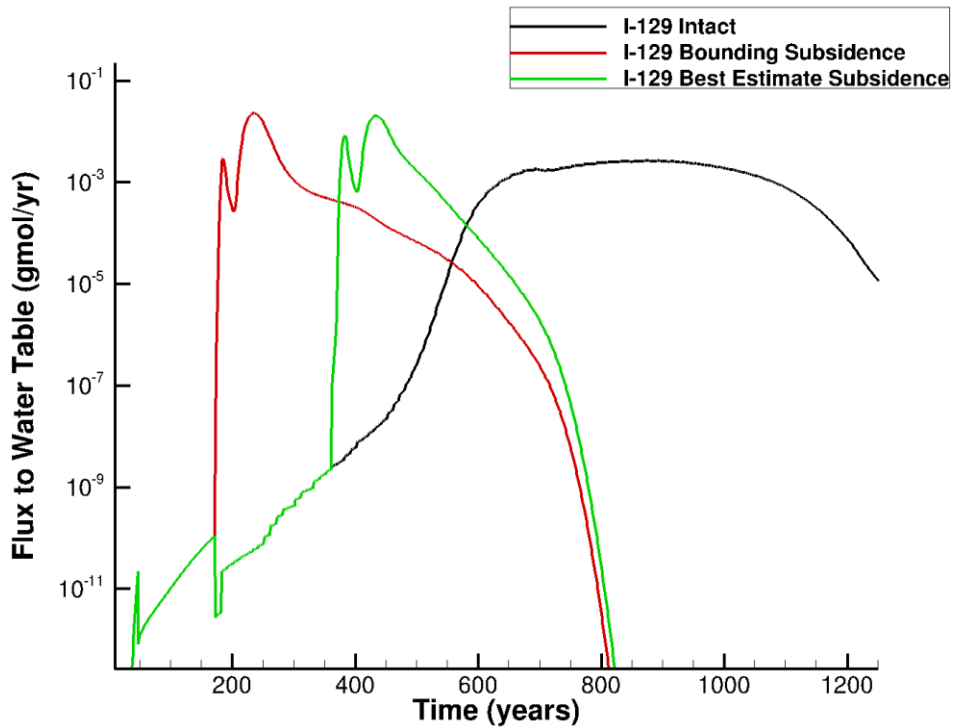


Figure 3-24. I-129 flux to the water table from CIG-4.

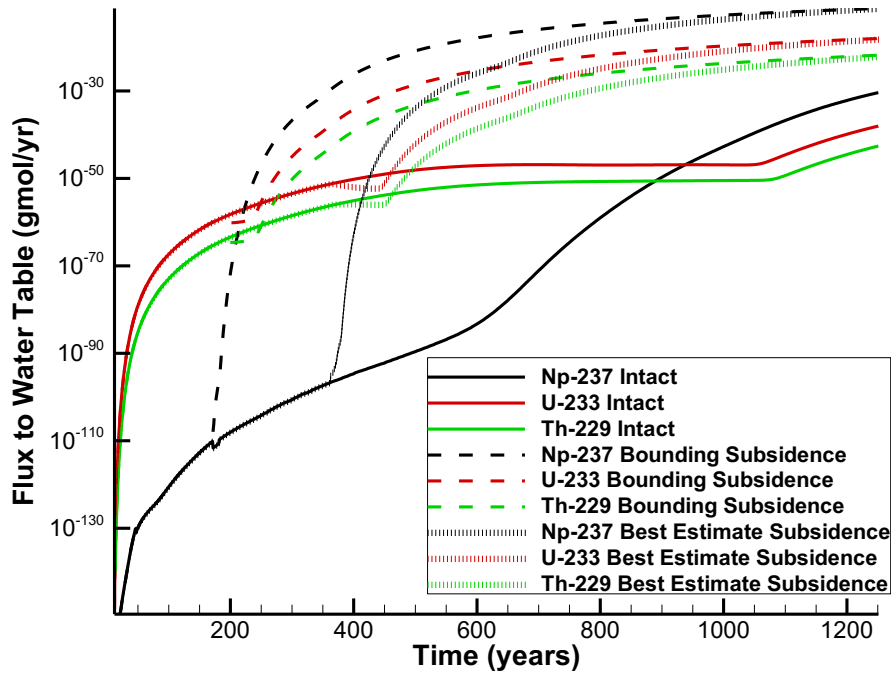


Figure 3-25. Np-237 flux to the water table from CIG-4.

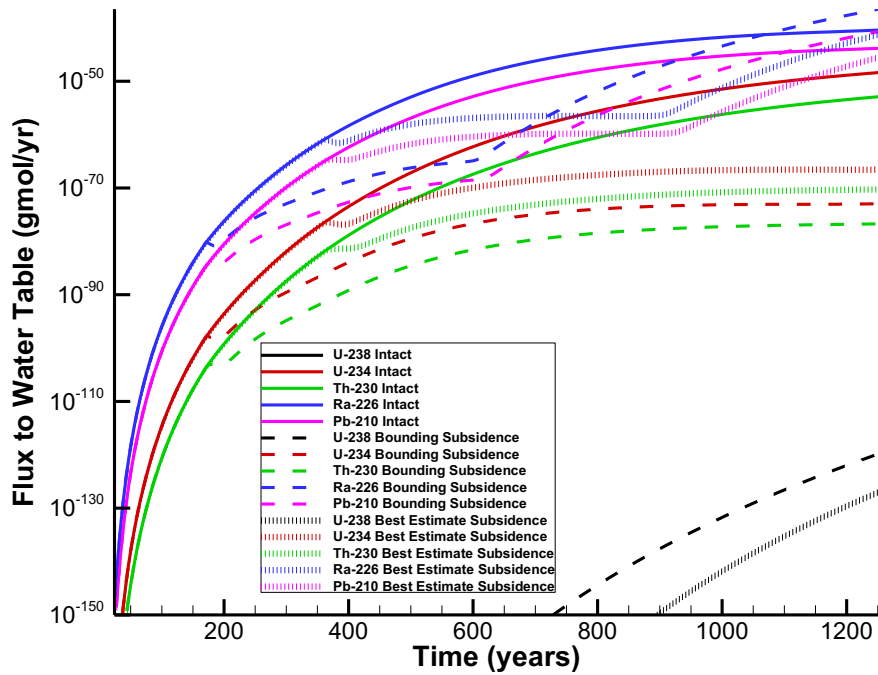


Figure 3-26. U-238 (and progeny) flux to the water table from CIG-4.

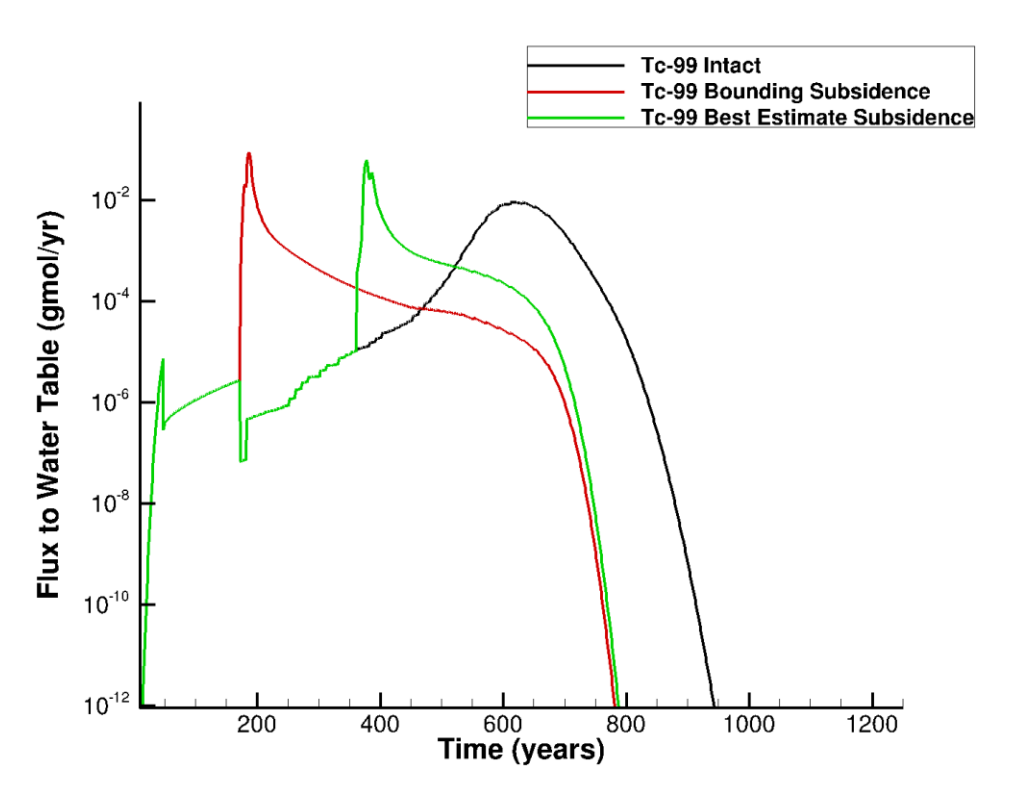


Figure 3-27. Tc-99 flux to the water table from CIG-4.

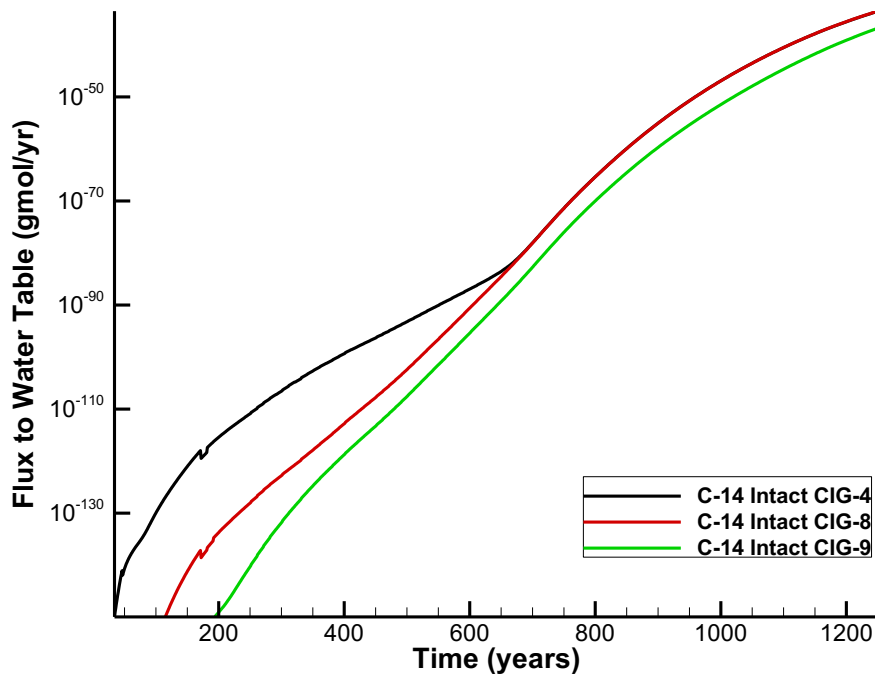


Figure 3-28. C-14 flux to the water table from CIG-4, -8, and -9.

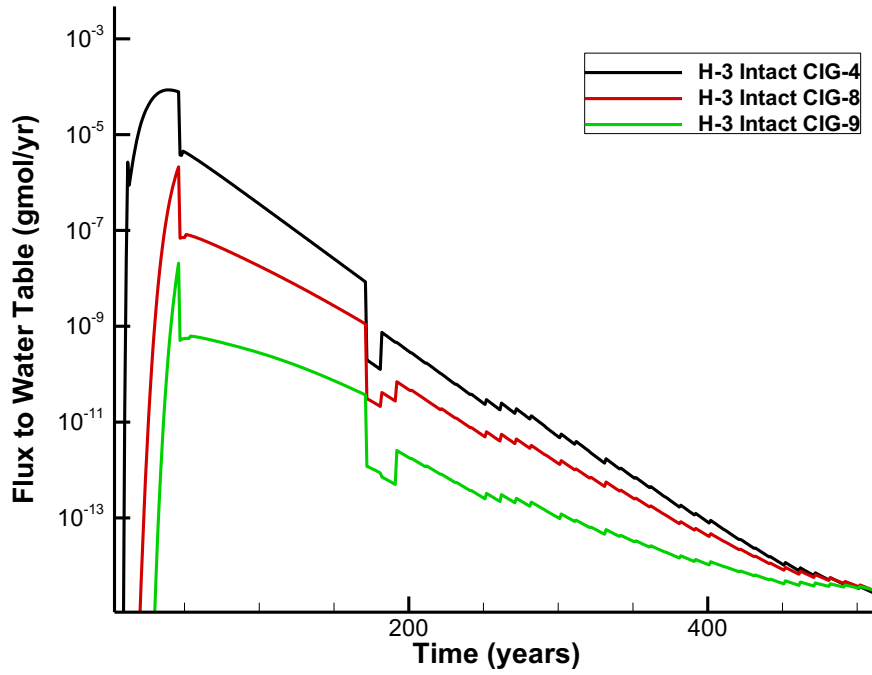


Figure 3-29. H-3 flux to the water table from CIG-4, -8, and -9.

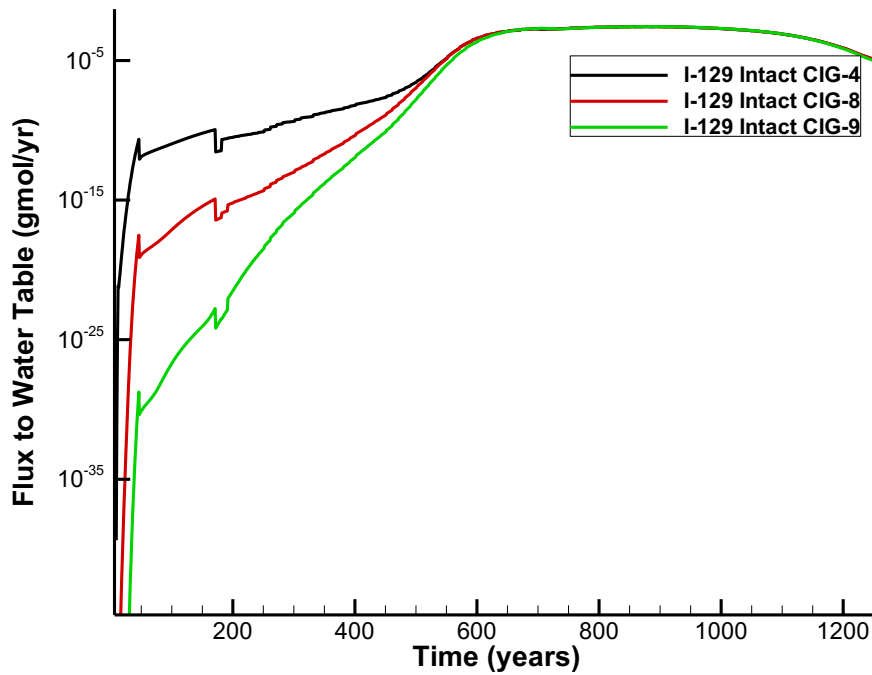


Figure 3-30. I-129 flux to the water table from CIG-4, -8, and -9.

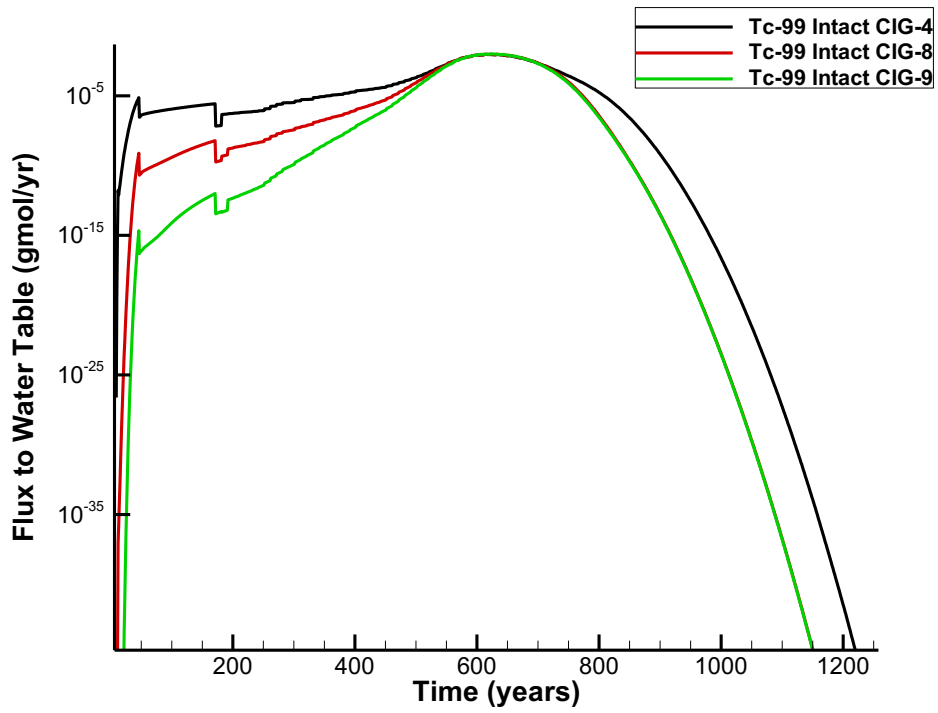


Figure 3-31. Tc-99 flux to the water table from CIG-4, -8, and -9.

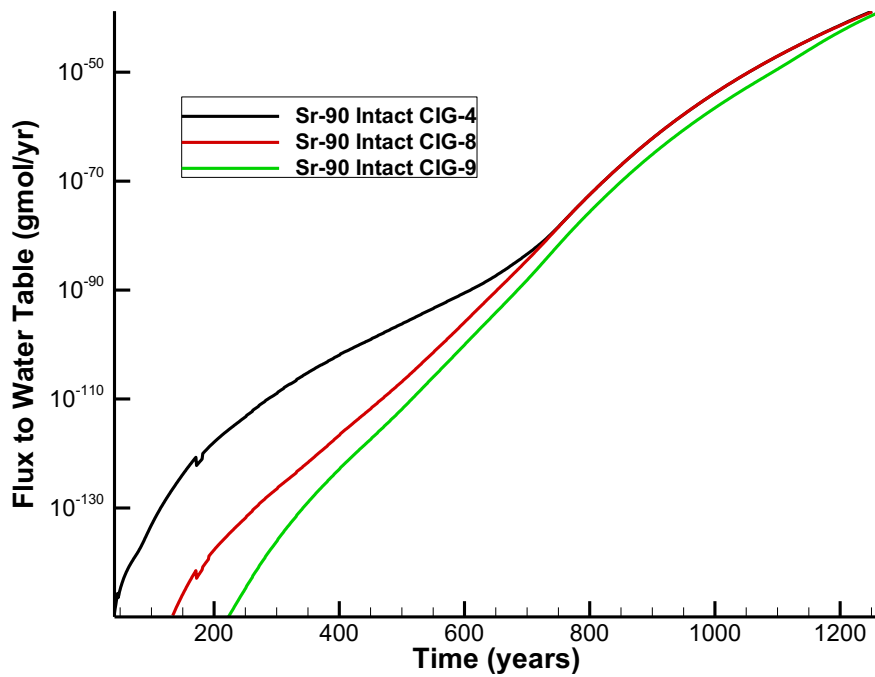


Figure 3-32. Sr-90 flux to the water table from CIG-4, -8, and -9.

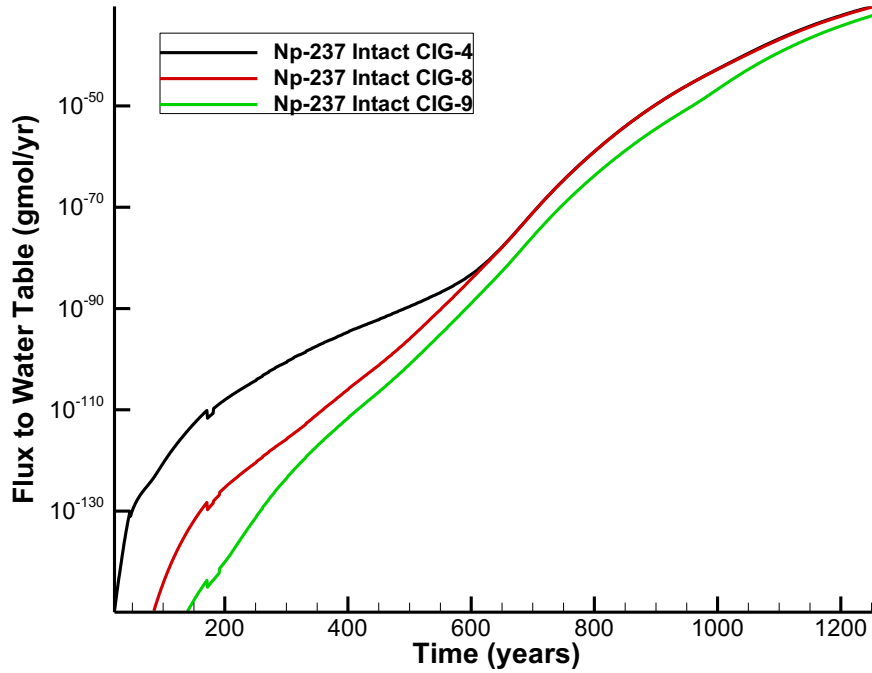


Figure 3-33. Np-237 flux to the water table from CIG-4, -8, and -9.

4.0 Conclusions

A conceptual model for the disposal units containing CIG waste has been developed. The models have been implemented within the PORFLOW software as they are intended to be used in the FY2022 ELLWF PA and preliminary results have been presented pending any changes to input parameters.

5.0 References

- ACRi, 2018. PORFLOW User's Manual, *Keyword Commands Version 6.42.9, Revision 0*. Analytical & Computational Research, Inc., Los Angeles, CA, April 23, 2018.
- Bagwell et al., 2017. L. A. Bagwell and P. L. Bennett, *Elevation of Water Table and Various Stratigraphic Surfaces beneath E Area Low Level Waste Disposal Facility*. SRNL-STI-2017-00301, Revision 1, Savannah River National Laboratory, Aiken, SC, August 2017.
- Danielson, 2019. T. L. Danielson, *PORFLOW Implementation of Vadose Zone Conceptual Model For Slit and Engineered Trenches in the E-Area Low Level Waste Facility Performance Assessment*. SRNL-STI-2019-00193, Revision 0, Savannah River National Laboratory, Aiken, SC, December 2019.
- Dyer, 2019. J. A. Dyer, *Infiltration Data Package for the E-Area Low-Level Waste Facility Performance Assessment*, SRNL-STI-2019-00363, Revision 0, Savannah River National Laboratory, Aiken, SC, November 2019.
- Kaplan, 2016. D. I. Kaplan, *Geochemical Data Package for Performance Assessment Calculations Related to the Savannah River Site*, SRNL-STI-2009-00473, Revision 1, Savannah River National Laboratory, Aiken, SC, July 2016.
- Nichols, 2019. R. L. Nichols, B. T. Butcher, *Hydraulic Properties Data Package for the E-Area Soils, Cementitious Materials, and Waste Zones - Update*, SRNL-STI-2019-00355, Revision 1, Savannah River National Laboratory, Aiken, SC, May 2020.
- Peregoy, 2006. W. Peregoy, *Structural Evaluation of Component-in-Grout Trenches*, T-CLC-E-00026, Revision 0, Washington Savannah River Company, Aiken, SC, August 2006.
- Phifer et al. 2009. M. A. Phifer, K. P. Crapse, M. Millings, M. G. Serrato, *Closure Plan for the E-Area Low-Level Waste Facility*, SRNL-RP-2009-00075, Revision 0, Savannah River National Laboratory, Aiken, SC, March 2009.

Distribution:

cj.bannochie@srnl.doe.gov
alex.cozzi@srnl.doe.gov
a.fellinger@srnl.doe.gov
samuel.fink@srnl.doe.gov
brenda.garcia-diaz@srnl.doe.gov
connie.herman@srnl.doe.gov
dennis.jackson@srnl.doe.gov
brady.lee@srnl.doe.gov
joseph.manna@srnl.doe.gov
daniel.mccabe@srnl.doe.gov
gregg.morgan@srnl.doe.gov
frank.pennebaker@srnl.doe.gov
amy.ramsey@srnl.doe.gov
william.ramsey@SRNL.DOE.gov
eric.skidmore@srnl.doe.gov
michael.stone@srnl.doe.gov
boyd.wiedenman@srnl.doe.gov
terry.foster@srnl.doe.gov
Records Administration (EDWS)

sebastian.aleman@srnl.doe.gov
tom.butcher@srnl.doe.gov
kerri.crawford@srs.gov
thomas.danielson@srnl.doe.gov
kenneth.dixon@srnl.doe.gov
james.dyer@srnl.doe.gov
peter.fairchild@srs.gov
scott.germain@srs.gov
luther.hamm@srnl.doe.gov
thong.hang@srnl.doe.gov
daniel.kaplan@srnl.doe.gov
dien.li@srs.gov
steven.mentrup@srs.gov
verne.mooneyhan@srs.gov
ralph.nichols@srnl.doe.gov
virginia.rigsby@srs.gov
jansen.simmons@srs.gov
ira.stewart@srs.gov
tad.whiteside@srnl.doe.gov
jennifer.wohlwend@srnl.doe.gov